Doctoral Dissertation

Regulation of intracellular localization and transcriptional activity of transcription activator Gln3 by dephosphorylation in *Saccharomyces cerevisiae*

Minori Numamoto

January 2015

Department of Biotechnology, Graduate School of Engineering

Osaka University

Table of contents

Chapter 1
General introduction

1-1 Protein phosphorylation

Phosphorylation is a common post-translational modification on proteins that provides functional diversity, such as protein interaction, intracellular localization, protein stability, and enzyme activity. Consequently, appropriate regulation on protein phosphorylation and dephosphorylation is very important for the majority of cellular processes. Protein phosphorylation and dephosphorylation are catalyzed by protein kinases and protein phosphatases, respectively. Interestingly, the number of phosphatases is three to five times smaller than that of kinases in eukaryotes, suggesting that the specificity of substrates in phosphatases is controlled not only by the variety of catalytic subunits but also by complicated regulation mechanisms including formation of the complex with the regulatory subunits.

Protein phosphatases in eukaryotes are classified into three families, namely phosphoprotein phosphatase (PPP), protein phosphatase Mg^{2+} or Mn^{2+}-dependent (PPM) and protein tyrosine phosphatase (PTP) families, based on the difference in their catalytic properties. PPP family phosphatases dephosphorylate specifically the phosphorylated serine and threonine of proteins (Zolnierowicz and Bollen 2000). PPP family phosphatases are further classified into PP1, PP2A, and PP2B (calcineurin) subfamily phosphatases. PPM family phosphatases, including PP2C subfamily phosphatases, act with Mg^{2+} or Mn^{2+} ion and also target phosphorylated serine and threonine residues of proteins. Unlike other phosphatases, PPM family phosphatases

are monomeric enzymes. PTP family phosphatases consist of two subfamilies, namely i) PTP that dephosphorylate phosphorylated tyrosine residues and ii) dual specificity phosphatases (DSP) that dephosphorylate phosphorylated tyrosine, serine and threonine residues of proteins.

1-2 Protein phosphatases in higher eukaryotes

In the higher eukaryotes *Homo sapiens*, 518 putative protein kinases and 137 putative protein phosphatases are identified (Lander et al. 2001; Venter et al. 2001). These putative protein kinases are classified into 90 tyrosine kinases and 428 serine and threonine kinases (Manning et al. 2002). In contrast, of the 137 protein phosphatases 107 are PTP family phosphatases, 17 are PPM family phosphatases and 13 are PPP phosphatases (Fig. 1) (Alonso et al. 2004; Shi 2009). Difference between the number of serine and threonine kinases (428) and seine and threonine phosphatases (30) suggests that substrate specificities of serine and threonine phosphatases of human are low compared with seine and threonine kinases. By contrast, it is assumed that PTP phosphatases (107) have high substrate specificities compared to serine and threonine phosphatases (30) since the number of PTP phosphatases (107) is similar to that of protein tyrosine kinases (90). On the other hand, more than 1,000 putative protein kinases and 122 putative protein phosphatases are identified from the genome database of the plant cells *Arabidopsis thaliana* (http://plantsp.genomics.purdue.edu/) (Ronne et al. 1991). Protein phosphatases compose 76 PPM family phosphatases, 27 PPP family phosphatases and 19 protein tyrosine phosphatases (Fig. 1) (Luan 2002; Schweighofer et al. 2004; Uhrig et al. 2013). Unlike human, protein tyrosine kinases

have not yet been identified in plant although the genome of *A. thaliana* encodes more than 1,000 serine and threonine kinases and dual-specificity kinases. Consistent with the absence of tyrosine kinases, the number of PTP phosphatases is very small (19). The number of serine and threonine phosphatases (103) is also small compared to serine and threonine kinases (>1,000). Therefore, it is thought that substrate specificities of protein phosphatases of plant are low compared with protein kinases. Plant PPM family phosphatases act as regulators of signal transduction pathway and are also involved in development (Schweighofer et al. 2004). It is thought that these phosphatases in higher eukaryotes may have been diverged from those of lower eukaryotes including the budding yeast *Saccharomyces cerevisiae* during the evolution. Therefore, we aim at understanding function of all protein phosphatases in *S.cerevisiae* in order to understand diversified function of protein phosphatases in higher eukaryotes.

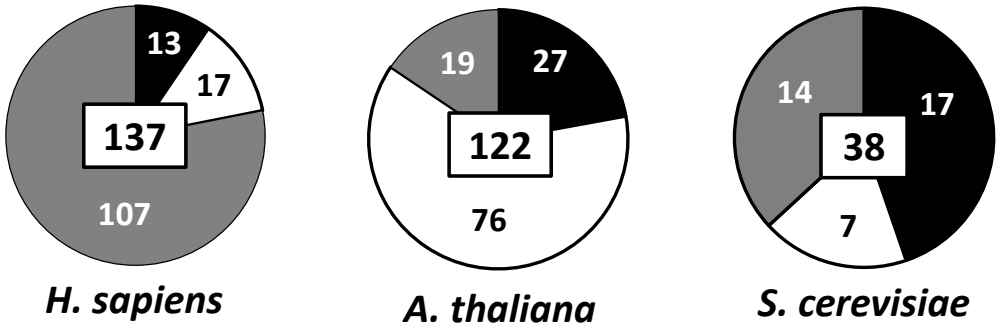

Fig. 1 Pie charts showing different families of protein phosphatases in *H. sapiens*, *A. thaliana*, and *S. cerevisiae*. The number of all protein phosphatases is shown in the center. PPP, PPM, and PTP family is depicted in black, white, and gray, respectively.

1-3 Protein phosphatases in *Saccharomyces cerevisiae*

In the genome of *S. cerevisiae*, a single-cell reference eukaryote, 117 protein kinases and 38 protein phosphatases have been estimated from the *Saccharomyces* genome sequence (http://www.yeastgenome.org/) (Table 1). Of the 38 protein phosphatases, 17 are PPP family phosphatases, 7 are PPM family phosphatases and 14 are PTP family phosphatases (Fig. 1). To elucidate the function of all protein phosphatases in yeast physiology, we started this project more than 15 years ago by constructing a series of disruptants for each of non-essential genes encoding the protein phosphatases (30 genes known at that time) and performed the approaches such as comprehensive growth phenotype analysis (Sakumoto et al. 1999; 2002). We also analyzed the gene expression profiling of those non-essential protein phosphatases gene disruptants and the function of individual protein phosphatases at molecular level (Hirasaki et al., 2008; 2010; 2012). These analyses led to the discovery of disruptants showing a variety of new phenotypes, including temperature sensitive and cation sensitive phenotypes. These works revealed that disruption of the *SIW14* gene increases sensitivity to caffeine (Sakumoto et al. 1999).

SIW14 was originally identified by synthetic interaction with *WHI2* that is required for full activation of the general stress response (Care et al. 2004). Although Siw14 was believed to encode a protein tyrosine phosphatase, Romá-Mateo et al. (2007, 2011) defined Siw14 as a homolog of plant and fungi atypical DSPs (PFA-DSPs) from bioinformatics, modeling analysis and biochemical tools. The analysis of the catalytic properties of PFA-DSPs suggests the specific physiological functions for Siw14. Siw14 is involved in actin organization and endocytosis in

response to nutrient starvation (Care et al. 2004). In addition to these cytoskeletal functions, Siw14 controls the phosphorylation, nuclear localization and transcriptional activity of Gln3 in response to caffeine (Hirasaki et al. 2008).

Table 1 Protein phosphatase genes in *S. cerevisiae*

Family/Subfamily	ORF/Gene	Function
PPP family		
PP1 subfamily	*YER133W/GLC7*	Involved in glycogen metabolism, sporulation and mitosis
	YML016C/PPZ1	Involved in regulation of potassium transport
	YDR436W/PPZ2	Functionally redundant with *PPZ1*
	YPL179W/SAL6	Regulating the mating response
PP2A subfamily	***YDL047W/SIT4***	Involved in the G1/S transition of the mitotic cycle
	YDL134C/PPH21	Involved in signal transduction and regulation of mitosis
	YDL188C/PPH22	Functionally redundant with *PPH21*
	YDR075W/PPH3	Regulating recovery from the DNA damage checkpoint
	YNR032W/PPG1	Involved in glycogen accumulation
PP2B subfamily (Calcineurin)	*YLR433C/CNA1*	Regulating ion homeostasis
	YML057W/CNA2	Functionally redundant with *CNA1*
Other	*YGR123C/PPT1*	Regulating Hsp90 chaperone
	YLL010C/PSR1	Involved in the general stress response
	YLR019W/PSR2	Functionally redundant with *PSR1*
	YMR277W/FCP1	Carboxy-terminal domain phosphatase
	YR004C/NEM1	Regulating nuclear growth
	YNL222W/SSU72	Transcription/RNA processing factor
PPP family		
PP2C subfamily	*YDL006W/PTC1*	Inactivating osmosensing MAPK cascade

	YER089C/PTC2	Dephosphorylating Cdc28, involved in HOG pathway
	YBL056W/PTC3	Functionally redundant with *PTC2*
	YBR125C/PTC4	A high-copy number suppressor of cnb1 mpk1 synthetic lethality
	YOR090W/PTC5	Involved in regulation of pyruvate dehydrogenase activity
	YCR079W/PTC6	Involved in mitophagy
	YHR076W/PTC7	Activating coenzyme Q6 biosynthesis
PTP family		
PTP subfamily	*YDL230W/PTP1*	Dephosphorylating a broad range of substrates in vivo, including Fpr3, a negative regulator of filamentation
	YDR208W/PTP2	Involved in the inactivation of mitogen-activated protein kinase (MAPK) during osmolarity sensing
	YER075C/PTP3	involved in the inactivation of mitogen-activated protein kinase (MAPK) during osmolarity sensing
	YPR073C/LTP1	Similarity to a phosphatase from bovine heart and human placenta
	YMR036C/MIH1	Involved in cell cycle control, regulating the phosphorylation state of Cdc28p
	YJR110W/YMR1	Involved in various protein sorting pathways
	YNL128W/TEP1	PTEN homolog
DSP subfamily	*YER028C/CDC14*	Involved in the cell cycle progression
	YBR276C/PPS1	A role in the DNA synthesis phase of the cell cycle
	YIR026C/YVH1	Involved in vegetative growth at low temperatures, sporulation, and glycogen accumulation
	YNL053W/MSG5	dephosphorylating Fus3
	YIL113W/SDP1	A paralog of *MSG5*
	YNL032W/SIW14	PFA-DSP, involved in actin organization and endocytosis
	YNL099C/OCA1	PFA-DSP, required for cell cycle arrest in response to oxidative damage of DNA

*Protein phosphatases focused on this thesis are shown in bold type.

1-4 Regulation of GATA transcriptional activator Gln3

S. cerevisiae can utilize a variety of compounds as nitrogen sources. In the presence of a preferred nitrogen source, such as glutamine, yeast cells repress transcription of genes required for the uptake and utilization of less preferred nitrogen sources. This physiological response is termed nitrogen catabolite repression (NCR)(Hofman-Bang 1999; Broach 2012; Conrad et al. 2014). Gln3 is one of the major transcription activators that regulate transcription of NCR-sensitive genes. It possesses a single zinc finger domain that has high similarity to the DNA binding domain of mammalian GATA factors, and binds to a GATA core sequence (5'-GATAAG-3') in the promoters of target genes to induce their transcription (Cooper 2002). When a preferred nitrogen source is available, Gln3 is restricted to the cytoplasm and, as a result, transcription of NCR-sensitive genes is not activated. In contrast, when the available nitrogen sources are comprised of non-preferred compounds such as proline, Gln3 translocates into the nucleus and activates transcription of NCR-sensitive genes (Cooper 2002; Conrad et al. 2014).

The intracellular localization and activity of Gln3 are regulated by the target of rapamycin complex 1 (TORC1) kinase (Fig. 2) (Beck & Hall 1999). In the presence of preferred nitrogen sources, Gln3 is phosphorylated in a TORC1 kinase-dependent manner and localizes to the cytoplasm. Inhibition of TORC1 kinase by rapamycin causes dephosphorylation of Gln3 through the PP2A family phosphatases Pph21 and Pph22 and the PP2A-like phosphatase Sit4. Details of these phosphatases are described in section 1-5. Dephosphorylation of Gln3 mediated by

Pph21, Pph22, and Sit4 results in the nuclear translocation of Gln3 and induction of the transcription of NCR-sensitive genes (Beck and Hall 1999; Bertram et al. 2000; Tate et al. 2006, 2009). However, the phosphorylation sites of Gln3 which are dephosphorylated by Sit4 and Pph21/Pph22 are not identified yet.

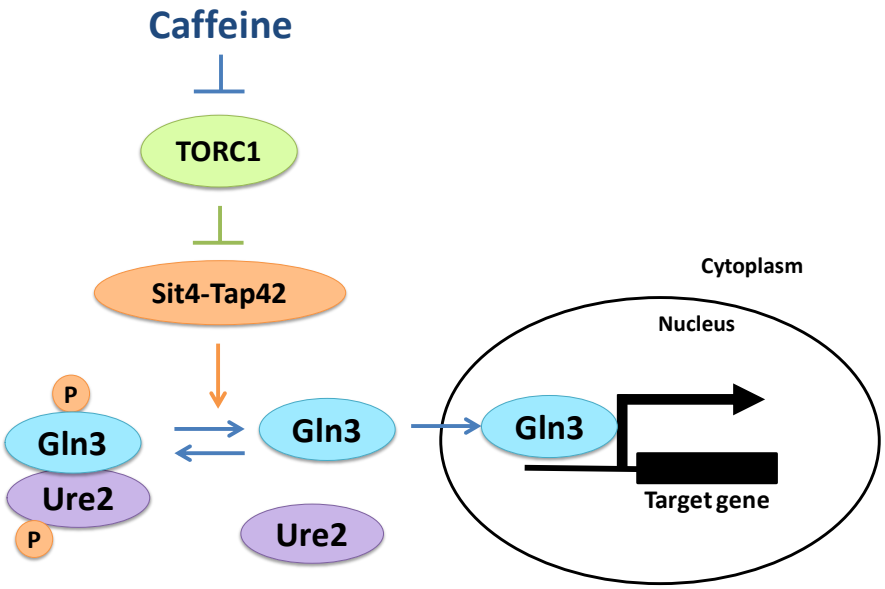

Fig. 2 Model for regulation of Gln3 in response to caffeine or rapamycin.

1-5 Physiological effects of caffeine in *S. cerevisiae*

Caffeine is the world's most widely consumed psychoactive drug. Caffeine affects a variety of cellular processes in mammals, plants and fungi, such as interfering with DNA repair (Selby and Sancar 1990), delaying cell cycle progression (Bode and Dong 2007), and modulating intracellular calcium homeostasis (McPhersonx et al. 1991). However, the mechanism by which caffeine triggers such pleiotropic effects is still largely unknown. In *S. cerevisiae*, growth sensitivity to caffeine is often associated with defects in components of Slt2 mitogen cell wall integrity pathway (Hampsey 1997). It is also thought that caffeine inhibits cyclic

adenosine monophosphate (cAMP), which subsequently affects protein kinase A (PKA) (Kuranda et al. 2006). Caffeine targets TORC1, and delays the cell cycle and extends the lifespan of cells (Reinke et al. 2006; Wanke et al. 2008) (Fig. 2), and causes the transcriptional induction of NCR-sensitive genes presumably through the same pathway as rapamycin treatment (Reinke et al. 2006; Kuranda et al. 2006).

1-6 PP2A phosphatases Pph21 and Pph22, and the PP2A-like phosphatases Sit4

Pph21 and Pph22 function by forming a heterotrimeric complex comprising a catalytic subunit, either Pph21 or Pph22; with a scaffolding protein (Tpd3); and one of two regulatory subunits (Cdc55 or Rts1), which impart different substrate specificities to the complex (Fig. 3A) (Sneddon et al. 1990; Ronne et al. 1991; van Zyl et al. 1992a; Shu et al. 1997). Pph21/Pph22 contributes to approximately half of the PP2A activity in the cell (Sneddon et al. 1990). Pph21/Pph22 plays a positive role for entry into mitosis (Lin and Arndt 1995) and a negative role at mitotic exit (Queralt et al. 2006). *SIT4* encodes catalytic subunit of PP2A-like phosphatase, but has the different function from those of Pph21 and Pph22. Sit4 is required for the G1/S transition (Sutton et al. 1991). Sit4 is structurally related to PP2A but does not interact with Tpd3, Cdc55, or Rts1. Sit4 exists mainly in complex with SAP proteins (Sap4, Sap155, Sap185, and Sap190), which determine the substrate specificity of Sit4 (Fig. 3B) (Luke et al. 1996). In addition to these main phosphatase complexes, Pph21, Pph22 and Sit4 exist in complex with another protein termed Tap42, and the functions of complex with Tap42 are regulated by TORC1 (Fig. 3C) (Di Como and Arndt 1996). Active TORC1 binds Tap42–Pph21, Tap42–Pph22, and Tap42–Sit4 complexes, forming an inactive complex

(Di Como and Arndt 1996; Wang et al. 2003). Inhibition of the TORC1 kinase by rapamycin or nitrogen depletion causes dissociation of the Tap42–phosphatase complex from TORC1, thereby activating the phosphatase in the cytoplasm (Yan et al. 2006). Nuclear localization of Gln3 after rapamycin treatment appears to be induced by the Tap42–phosphatase complexes because inactivation of Tap42 significantly weakens the induction of NCR gene expression by rapamycin (Düvel et al. 2003). In addition to the Tap42–phosphatase complexes, it has been also reported that rapamycin-induced nuclear localization of Gln3 requires all PP2A components—that is, Pph21/Pph22, Tpd3, Cdc55, and Rts1 (Georis et al. 2009).

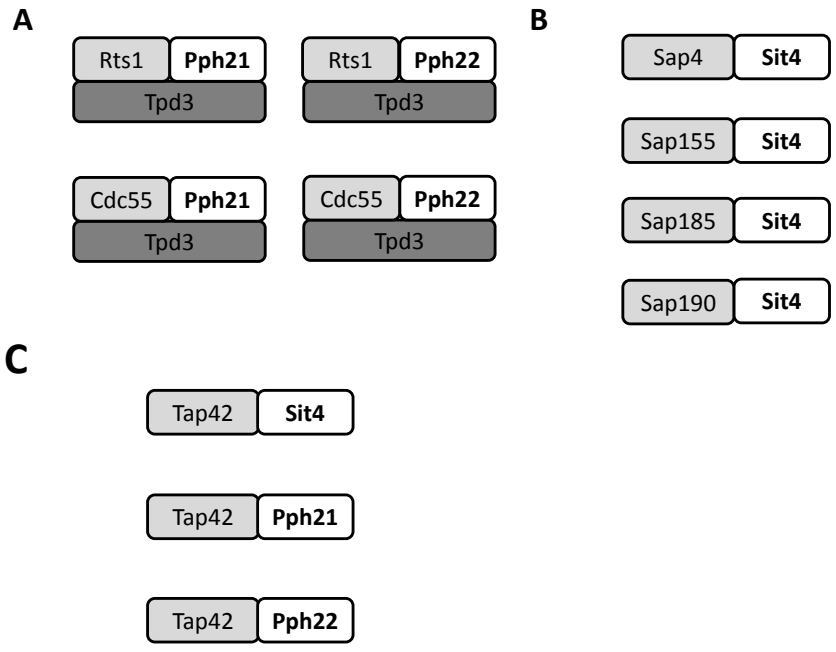

Fig. 3 Multiple complexes of Pph21, Pph22, and Sit4 in *S. cerevisiae*. (A) PP2A complex is composed of Pph21 or Pph22 as catalytic subunit, Tpd3 as scaffolding subunit, and Rts1 or Cdc55 as regulatory subunit. (B) Sit4 specific complex is composed Sit4 of catalytic subunit and Sap4, Sap155, Sap185 or Sap190 as regulatory subunit. (C) Sit4, Pph21, or Pph22 form the complex with Tap42. The details are described in the text.

1-7 Objectives of the study

Although dephosphorylation of Gln3 by caffeine treatment leads to nuclear translocation of Gln3 and subsequent transcription of NCR-sensitive genes, the phosphorylation sites of Gln3 and the mechanisms by which protein phosphatases Siw14, Pph21, Pph22, and Sit4 control the intracellular localization and transactivation of Gln3 are unknown. This objective of this study is to elucidate the mechanism by which Siw14 controls the intracellular localization and transactivation of Gln3 in response to caffeine.

In Chapter 1 of this thesis, I summarized the background information for this study: the regulation mechanisms of GATA transcriptional factor Gln3 and protein phosphatases, Siw14, Pph21, Pph22, and Sit4. In Chapter 2, I aimed to gain an understanding of the role for Siw14 in the caffeine-induced nuclear translocation of Gln3. Siw14 was found to control the caffeine-induced nuclear translocation and phosphorylation of Gln3 through PP2A phosphatases Pph21 and Pph22. In Chapter 3, I focused on the phosphor-acceptor sites in two nuclear localization signals (NLS-K and NLS-C) and the nuclear export signals (NES) in Gln3. From the analysis of transcription of target genes with the point mutants in these regions, I found that transcriptional activity of Gln3 is regulated by dephosphorylation of Thr-339 and Ser-344 in NES region, and Ser-344, Ser-347 and Ser-355 in NLS-K region although these mutations have no effects on the intracellular localization of Gln3. Finally, in Chapter 4, I discuss the mechanism by which dephosphorylation of Gln3 controls the intracellular localization and transcriptional activity in association with the present findings.

Chapter 2

The protein phosphatase Siw14 controls caffeine-induced nuclear localization and phosphorylation of Gln3 via the PP2A protein phosphatases Pph21 and Pph22 in *S. cerevisiae*

2-1 Introduction

The *S. cerevisiae* Siw14 participates in regulation of the phosphorylation and intracellular localization of Gln3. In Δ*siw14* cells, the phosphorylation level of Gln3 is decreased and the nuclear localization of Gln3 is stimulated by caffeine (Hirasaki et al. 2008). However, the mechanism by which Siw14 controls the localization and function of Gln3 remains unclear, although the nuclear localization of Gln3 is known to be induced by activation of the PP2A phosphatases (PP2As) Pph21 and Pph22, and the PP2A-like phosphatase Sit4 (Tate et al. 2006, 2009).

The aim of Chapter 2 is to gain an understanding of how Siw14 participates in regulation of Gln3 phosphorylation/dephosphorylation and intercellular localization. In this chapter, I showed that the increased nuclear localization of Gln3 in response to caffeine caused by disruption of the *SIW14* gene was dependent on the Sit4 and PP2A phosphatases. I also showed that decreased phosphorylation of Gln3 caused by disruption of the *SIW14* gene was completely suppressed by deletion of both *PPH21* and *PPH22*, but only partially suppressed by deletion of *SIT4*. Taking these results together, I concluded that Siw14 functions upstream of Pph21 and Pph22 as an inhibitor of the phosphorylation and localization of Gln3, and that Sit4 acts independently of Siw14.

2-2 Materials and methods

2-2-1 Strains, media and general methods

The yeast strains used in this study are listed in Table 2. Yeast strains were grown at 30°C using standard rich medium (YPDA, Difco) or SC dropout medium. YPDA medium containing 300 μg/ml of G418 sulfate (Calbiochem) or 200 μg/ml of Zeocin (Invitrogen) was used to select strains carrying the *KanMX4* gene or the Zeocin resistance gene, respectively. For the caffeine treatment, cells were shifted to fresh YPDA medium supplemented with the caffeine concentrations indicated in the figures (Wako Pure Chemical Industries). The *Escherichia coli* strains used as a source of plasmids, including SHB3008 for p3008 (*CgLEU2*) (Sugiyama et al. 2005) and SHB3296 for p3296 (*loxP*::Zeocin^{R}::*loxP*), were cultivated in LB medium containing 50 μg/ml of ampicillin at 37°C (Sambrook, E.F. Fritsch 1989). Single, double and triple gene disruptants were constructed by using a PCR-mediated gene disruption method as described (Sakumoto et al. 1999). Confirmation PCR using specific primers was done to verify the correct disruption of genes. The primers used in the construction and confirmation of the different kinds of disruptants are listed in Table 3.

Table 2 Strains used in Chapter 2

Name	Genotype	Source
BY4742	*MATα leu2Δ0 his3Δ1 lys2Δ0 ura3Δ0*	Invitrogen
MH117	*MATα leu2Δ0 his3Δ1 lys2Δ0 ura3Δ0 GLN3-MYC*^{13}*::CgHIS3*	Hirasaki et al., 2008
MH118	*MATα leu2Δ0 his3Δ1 lys2Δ0 ura3Δ0 Δsiw14::KanMX4 GLN3-MYC*^{13}*::CgHIS3*	Hirasaki et al., 2008
MN42	*MATα leu2Δ0 his3Δ1 lys2Δ0 ura3Δ0 Δsit4::CgLEU2 GLN3-MYC*^{13}*::CgHIS3*	*SIT4* disruptant of MH117
MN45	*MATα leu2Δ0 his3Δ1 lys2Δ0 ura3Δ0 Δsiw14::KanMX4 Δsit4::CgLEU2 GLN3-MYC*^{13}*::CgHIS3*	*SIT*4 disruptant of MH118
MN80	*MATα leu2Δ0 his3Δ1 lys2Δ0 ura3Δ0 Δpph21::CgLEU2 GLN3-MYC*^{13}*::CgHIS3*	*PPH21* disruptant of MH117
MN81	*MATα leu2Δ0 his3Δ1 lys2Δ0 ura3Δ0 Δsiw14::KanMX4 Δpph21::CgLEU2 GLN3-MYC*^{13}*::CgHIS3*	*PPH21* disruptant of MH118
MN82	*MATα leu2Δ0 his3Δ1 lys2Δ0 ura3Δ0 Δpph22::CgLEU2 GLN3-MYC*^{13}*::CgHIS3*	*PPH22* disruptant of MH117
MN83	*MATα leu2Δ0 his3Δ1 lys2Δ0 ura3Δ0 Δsiw14::KanMX4 Δpph22::CgLEU2 GLN3-MYC*^{13}*::CgHIS3*	*PPH22* disruptant of MH118
MN122	*MATα leu2Δ0 his3Δ1 lys2Δ0 ura3Δ0 Δpph21::loxP*-Zeocin^{R}-*loxP Δpph22::CgLEU2 GLN3-MYC*^{13}*::CgHIS3*	*PPH21* disruptant of MN82
MN123	*MATα leu2Δ0 his3Δ1 lys2Δ0 ura3Δ0 Δsiw14::KanMX4 Δpph21::loxP*-Zeocin^{R}-*loxP Δpph22::CgLEU2 GLN3-MYC*^{13}*::CgHIS3*	*PPH21* disruptant of MN83
MN84	*MATα leu2Δ0 his3Δ1 lys2Δ0 ura3Δ0 Δtpd3::CgLEU2 GLN3-MYC*^{13}*::CgHIS3*	*TPD3* disruptant of MH117
MN85	*MATα leu2Δ0 his3Δ1 lys2Δ0 ura3Δ0 Δsiw14::KanMX4 Δtpd3::CgLEU2 GLN3-MYC*^{13}*::CgHIS3*	*TPD3* disruptant of MH118
MN37	*MATα leu2Δ0 his3Δ1 lys2Δ0 ura3Δ0 NPR1-MYC*^{13}*::CgHIS3*	Derived from BY4742
MN74	*MATα leu2Δ0 his3Δ1 lys2Δ0 ura3Δ0 Δsiw14::KanMX4 NPR1-MYC*^{13}*::CgHIS3*	*SIW14* disruptant of MN37
MN76	*MATα leu2Δ0 his3Δ1 lys2Δ0 ura3Δ0 Δsit4::CgLEU2 NPR1-MYC*^{13}*::CgHIS3*	*SIT4* disruptant of MN37

MN77	*MATα leu2Δ0 his3Δ1 lys2Δ0 ura3Δ0 Δsiw14*::*KanMX4* Δ*sit4*::*CgLEU2 NPR1-MYC*^{13}::*CgHIS3*	*SIT4* disruptant of MN74

Table 3 Primers used in Chapter 2

Primer	Primer sequence
SIT1 KF	5’-TGAAATACTATTGAAGCTCAAAAACATCCATAATAAAAGGAACAATAACAGTTCGTACGCTGCAG-3’
SIT1 KR	5’-AAGTAGGTTCCAGATCCTCATCGACCTTCATTACACTCGCGACATTACCAGCCACTAGTGGAT CT-3’
SIT1 CF	5’-GGGGAATAACACAGCCGCGG-3’
SIT1 CR	5’-ATGGTTATGCTTTTCTGCCT-3’
PPH21 KF	5’-GGATATAAATTATCGCATAAAACAATAAACAAAAAGAAAAATGCTTCGTACGCTGCAG-3’
PPH21 KR	5’-TAATCTGGCGTCTTTCTGCTGACGCTAGGTTCACCTGGTCGCCACTAGTGGATCT-3’
PPH21 CF	5’-GCCCCTATTTAGTTCATAGTGG-3’
PPH21 CR	5’-TGGGGAGGAAAAAAAGCCTC-3’
PPH22 KF	5’-TTATTGGCACTTCTGTATAACTGGCTTTCATTCGAAAAAAATGCTTCGTACGCTGCAG-3’
PPH22 KR	5’-AAGAAATAATCCGGTGTCTTCCTGGTGACGGTTGGTTCACGCCACTAGTGGATCT-3’
PPH22 CF	5’-GTGTTCGAACAAGAACACGC-3’
PPH22 CR	5’-GCGTGAGGAGTGAACTATAC-3’
TPD3 KF	5’-ATTATCGAAGAATAATTGAGTGGTCAGAAAGGAGCGAAATATGCTTCGTACGCTGCAG-3’
TPD3 KR	5’-TATCAATTTTTTAAAAGTTCTTGACATTCTGCCAAACTTTGCCACTAGTGGATCT-3’
TPD3 CF	5’-TACGAAGGAAGGCAGATAGC-3’
TPD3 CR	5’-GTGGAGGCGGAAATCAATGT-3’

2-2-2 Indirect immunofluorescence microscopy

Cells grown to mid-log phase (OD_{660} = 0.5) in YPDA medium were shifted to

YPDA medium containing caffeine and incubated at 30°C. Cells were fixed with formaldehyde (at final concentration of 3.7%) for 45 min. Following fixation, the samples were washed and resuspended in 0.1 M potassium phosphate buffer (pH 6.5) containing 1.2 M sorbitol and 0.05 M $MgCl_2$. The cell wall was digested by using 10 μg/ml of Zymolyase 100T (Seikagaku Biobusiness) in the presence of β-mercaptoethanol. The cells were then plated onto slides coated with 0.5 mg/ml of poly-lysine (Poly-$_L$-lysine hydrobromide, Sigma Aldrich) and incubated overnight at 4°C in phosphate buffer (pH 7.4) containing 1% bovine serum albumin (Wako Pure Chemical Industries). Antibody incubations and subsequent washes were performed with this phosphate buffer. Primary antibody labeling of Gln3-Myc[13] was performed using 9E10 (c-Myc) monoclonal antibody (Santa Cruz) at a dilution of 1:500, followed by secondary labeling with CyTM3-conjugated AffiniPure sheep anti-mouse IgG antibody (Jackson ImmunoResearch) at a dilution of 1:500. DNA was stained for fluorescence observation using 4',6-diamidino-2-phenylindole (DAPI) (Vector). Cells were observed by fluorescence microscopy (BX61, Olympus) and photographed with a CCD camera (CCD-EX1, Universal Imaging Corporation, USA).

Approximately 100 cells were counted and classified into one of three groups according to the localization of Gln3-Myc[13]: cytoplasmic (only cytoplasmic fluorescence), partially nuclear (fluorescence in the cytoplasm and weak fluorescence in the nucleus) and nuclear (strong fluorescence in the nucleus). Representative images demonstrating the differences among these groups are shown in Fig. 4A.

2-2-3 Immunoblotting

Protein extracts for immunoblotting were prepared by trichloroacetic acid (TCA) methods using cells grown to mid-log phase (OD_{660} = 0.5) at 30°C in YPDA medium and then incubated in YPDA medium containing 5 mM caffeine for 10 min. Cells were resuspended in 0.2775 N NaOH and incubated on ice for 10 min. Next, 150 μl of 55% TCA was added to the cell suspension, which was then incubated on ice for 10 min. After centrifugation, precipitates were resuspended in HU buffer: 8 M Urea, 5% SDS, 200 mM Tris–HCl (pH 6.8), 0.1 mM EDTA, 15mg/ml dithiothreitol, and bromophenol blue, and incubated at 65°C for 15 min. Total protein concentration was measured with a Quanti-iT^{TM} Protein Assay Kit (Invitrogen), and samples containing 20 μg of protein were used for SDS–PAGE. Gln3-Myc[13] was detected with horseradish peroxidase (HRP)-conjugated anti-mouse monoclonal IgG_1 (c-Myc Antibody [9E10] HRP: Santa Cruz) at a dilution of 1: 1000 using ECL western lightning chemiluminescence (Perkin Elmer).

2-2-4 Immunoprecipitation and phosphatase treatment

Crude protein extracts were prepared with lysis buffer: 25 mM Tris–HCl (pH 8.0), 100 mM NaCl, 10 mM $MgCl_2$, 0.1% Triton X-100, 1 mM EDTA, 1 mM EGTA, 10% glycerol, 10 mM PMSF, protease inhibitor cocktail (Sigma Aldrich), and phosphatase inhibitor cocktail (Nacalai tesque). For immunoprecipitation, 1 mg of protein extract was used with 5 μg of anti-c-myc (9E10: Santa Cruz) and 0.45 mg of Dynabeads protein G (life technologies). Phosphatase treatment was performed using 400 units of Lambda protein phosphatase (Biolabs inc.) or 400 units of Lambda protein

phosphatase plus phosphatase inhibitor cocktail for 30 min at 30ºC. Samples were eluted in HU buffer for loading onto the gel.

2-3 Results

2-3-1 Disruption of *SIW14* increases the proportion of nuclear Gln3-Myc^{13} localization in response to caffeine

In our previous study, we discovered that Siw14 controls nuclear localization of Gln3 (Hirasaki et al. 2008). To evaluate the role of Siw14 in Gln3 localization in more detail, I observed the distribution of Gln3-Myc^{13} between the cytoplasm and the nucleus under various caffeine concentrations both in wild-type and in Δ*siw14* cells. Unexpectedly, a significant portion of Gln3-Myc^{13} was localized to the cytoplasm, as well as wild-type cells, in the absence of caffeine in Δ*siw14* cells (Fig. 4A), which differs from previous findings (Hirasaki et al. 2008). One possibility for this difference might be inhomogeneity in the antibody staining of Gln3-Myc^{13} in the previous study. Therefore, because quantitative analysis of the intracellular localization of Gln3-Myc^{13} was not performed in the previous study, I classified the cells into three groups based on the intracellular localization of Gln3-Myc^{13}, as described in 'Materials and methods' section, and counted the number of cells in each group (Fig. 4B and C). At low concentrations of caffeine (2–14 mM), Δ*siw14* cells exhibited a higher proportion of nuclear and partial nuclear localization of Gln3-Myc^{13} as compared with wild-type cells, particularly at 5 mM caffeine ~88% of Δ*siw14* cells showed nuclear or partial nuclear localization of Gln3-Myc^{13} versus ~18% of wild-type cells (Fig. 4B). In contrast, Gln3-Myc^{13} was localized in the cytoplasm in both wild-type and Δ*siw14* cells in the absence of caffeine (0 mM).

To gain more insight into the temporal transition in Gln3 localization between the cytoplasm and the nucleus in response to caffeine, I observed the intracellular localization of Gln3-Myc^{13} over a period of 60 min after a shift to 5 mM caffeine medium (Fig. 4C). Before caffeine treatment (0 min.), Gln3-Myc^{13} was localized in the cytoplasm in both wild-type and Δ*siw14* cells. Approximately 60% of wild-type cells showed nuclear or partial nuclear localization of Gln3-Myc^{13} at 10 min after the shift to caffeine medium. Subsequently, the percentage of cells with nuclear or partial nuclear localization of Gln3-Myc^{13} gradually decreased, and nearly all cells displayed only cytoplasmic localization of Gln3-Myc^{13} within 40 min of the shift to caffeine medium. In contrast, more than 80% of Δ*siw14* cells showed nuclear or partial nuclear localization of Gln3-Myc^{13} within 5 min and this distribution remained until 20 min. Sixty minutes after the shift to caffeine medium, ~10% of Δ*siw14* cells still showed partial nuclear localization of Gln3-Myc^{13} (Fig. 4C). From these results, I conclude that Siw14 inhibits the nuclear translocation of Gln3-Myc^{13} in the presence of caffeine.

2-3-2 Disruption of *SIT4* suppresses nuclear Gln3-Myc^{13} localization in response to caffeine in wild-type and Δ*siw14* cells.

In previous studies, nuclear translocation of Gln3 was induced by activation of the PP2A-like phosphatase Sit4 (Beck and Hall 1999; Tate et al. 2006). To reveal the genetic epistasis between *SIW14* and *SIT4*, I investigated whether the nuclear localization of Gln3-Myc^{13} that occurs in response to caffeine in wild-type and Δ*siw14* cells was dependent upon Sit4. As reported by Tate and Cooper (2007), the nuclear

translocation of Gln3-Myc^{13} in response to caffeine was inhibited by the disruption of *SIT4* (Fig. 5) in both type of cells. Therefore, these results indicate that the increased nuclear localization of Gln3-Myc^{13} in response to caffeine caused by disruption of the *SIW14* gene is dependent upon Sit4.

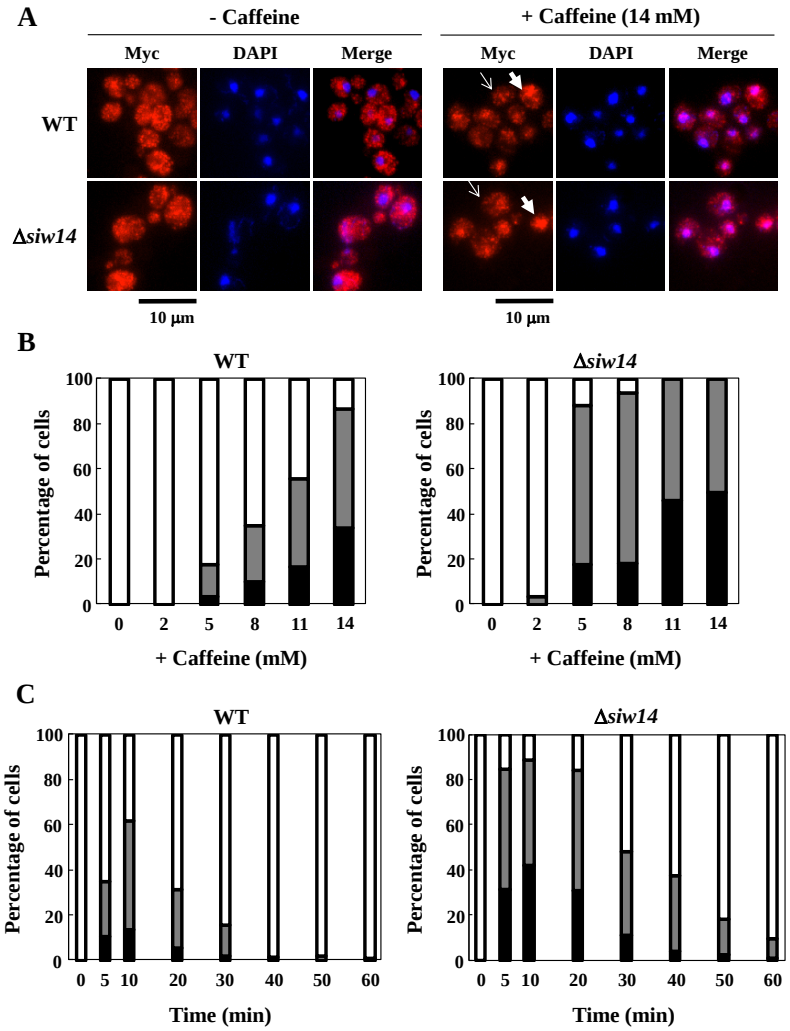

Fig. 4 Disruption of *SIW14* increases the proportion of Gln3-Myc^{13} localized in the nucleus in response to caffeine. (A) Wild-type (MH117) and Δ*siw14* (MH118) cells were grown to mid-log phase (OD_{660} = 0.5) in YPDA medium and then shifted to YPDA medium or YPDA medium containing 14 mM caffeine for 15 min. Gln3-Myc^{13} localization was visualized by indirect immunofluorescence microscopy. Nuclear DNA was stained with DAPI. Thick and thin arrows point to cells with nuclear localization and partial nuclear localization of Gln3, respectively.

(B) Wild-type (MH117) and Δ*siw14* (MH118) cells were grown to mid-log phase (OD_{660} = 0.5) in YPDA medium and then shifted to YPDA medium containing 0–14 mM caffeine for 15 min. Gln3-Myc[13] localization was visualized by indirect immunofluorescence microscopy. According to Gln3-Myc[13] localization, cells were classified into three groups: nuclear (black), partially nuclear (gray), and cytoplasmic (white). Approximately 100 cells were counted and the percentage of cells in each group is shown. (C) Wild-type (MH117) and Δ*siw14* (MH118) cells were grown to mid-log phase (OD_{660} = 0.5) in YPDA medium and then shifted to YPDA medium containing 5 mM caffeine for 1 h. Samples were removed at the indicated times, and analyzed as in panel (B).

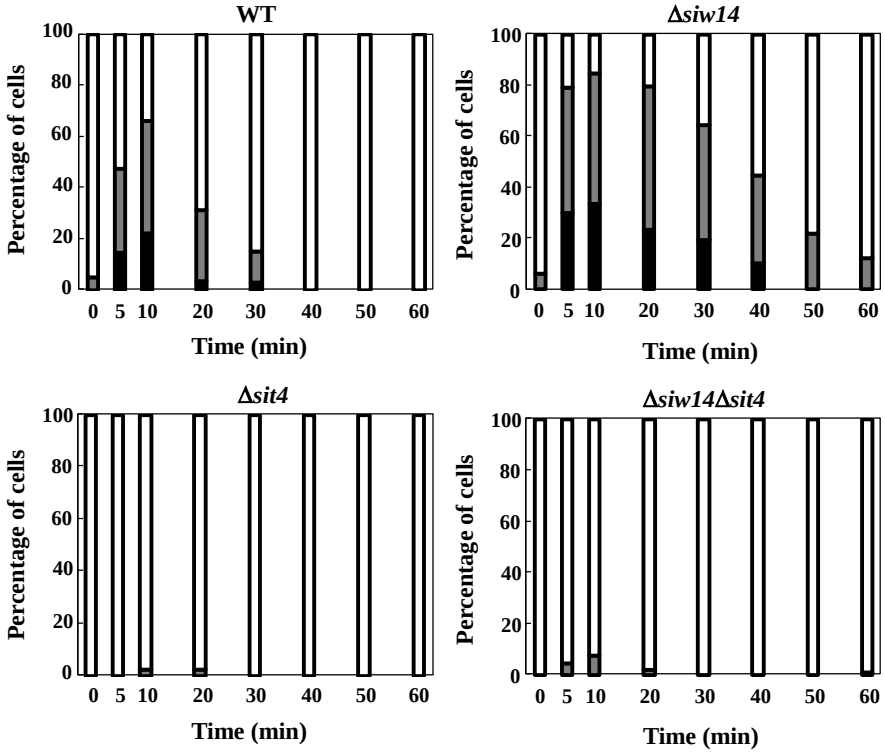

Fig. 5 Disruption of *SIT4* inhibits nuclear Gln3-Myc[13] localization in wild-type and Δ*siw14* cells in response to caffeine. Wild-type (MH117), Δ*siw14* (MH118), Δ*sit4* (MN42), and Δ*siw14*Δ*sit4* (MN45) cells were grown to mid-log phase (OD_{660} = 0.5) in YPDA medium, and then incubated in YPDA medium containing 5 mM caffeine for 1 h. Gln3-Myc[13] localization was visualized by indirect immunofluorescence microscopy. The experimental conditions and the data presentation are the same as in Fig. 4.

2-3-3 Decreased Gln3 phosphorylation due to disruption of *SIW14* is in part dependent on Sit4

Gross phosphorylation and localization of Gln3 are often correlated with one another (Beck and Hall 1999; Bertram et al. 2000). I therefore examined the phosphorylation status of Gln3-Myc^{13} under caffeine treatment (Fig. 6). As shown by Hirasaki et al. (2008), the gel mobility of Gln3-Myc^{13} in wild-type cells increased after a shift to caffeine medium (Fig. 6A, lane 1, arrow c; and lane 4, arrow b). To confirm whether the shift was due to a change in phosphorylation levels, I treated Gln3-Myc^{13} immunoprecipitates with lambda protein phosphatase. Phosphatase treatment of immunoprecipitates led to faster gel mobility, and phosphatase inhibitor completely blocked this increase (Fig. 6A, lane 1 and 3, arrow c; lane 2, arrow a). Next, I investigated whether the increase in gel mobility induced by caffeine was caused by dephosphorylation. If caffeine treatment induces dephosphorylation of Gln3, then phosphatase treatment of immunoprecipitates from an extract prepared after a shift to caffeine medium should show the same gel mobility of Gln3-Myc^{13} as that from an extract without caffeine treatment. The result (Fig. 6A, lane 2 and 5, arrow a) was consistent with my hypothesis that the increase in gel mobility induced by caffeine (Fig. 6A, lane 1, arrow c; lane 4, arrow b) was caused by dephosphorylation. I also confirmed that the gel mobility of Gln3-Myc^{13} was increased in Δ*siw14* cells relative to that in wild-type even before caffeine treatment (Fig. 6B, lane 1, arrow c versus lane 4, arrow b; Fig. 6D, lane 2, arrow c versus lane 3, arrow a–c), as shown in a previous report (Hirasaki et al. 2008). The gel mobility of Gln3-Myc^{13} treated with phosphatase in Δ*siw14* cells was the same as that in wild-type cells treated with

phosphatase in the absence of caffeine (Fig. 6B, lane 2 and 5, arrow a), suggesting that disruption of the *SIW14* gene partially decreases the phosphorylation level of Gln3-Myc^{13}. These results imply that Siw14 controls phosphorylation of Gln3 via activation of protein kinases or inhibition of protein phosphatases but not by direct dephosphorylation of Gln3-Myc^{13} because, if Siw14 were able to dephosphorylate Gln3 directly, the band shift would be reversed as *SIW14* itself encodes a protein phosphatase. Gln3-Myc^{13} prepared from extracts in the presence of rapamycin, which is well known to induce dephosphorylation of Gln3, also showed faster mobility (Fig. 6C, lane 1 and 3, arrow a). Therefore, I used this form of Gln3-Myc^{13} as a control for the dephosphorylated Gln3-Myc^{13} in subsequent experiments.

The dephosphorylation of Gln3-Myc^{13} induced by caffeine and rapamycin is known to be dependent on Sit4 phosphatase activity (Beck and Hall 1999; Tate and Cooper 2007). Therefore, I examined whether the decrease in Gln3-Myc^{13} phosphorylation in Δ*siw14* cells was caused by the phosphatase function of Sit4. The level of Gln3-Myc^{13} phosphorylation in Δ*sit4* cells was similar to that in wild-type cells in the absence of caffeine (Fig. 6D, lane 2 and 5, arrow c). However, in the presence of caffeine, phosphorylation level of Gln3-Myc^{13} in Δ*sit4* cells was higher than that of wild-type cells (Fig. 6D, lane 8, arrow b versus lane 11, arrow d). Interestingly, the phosphorylation level of Gln3-Myc^{13} in Δ*siw14*Δ*sit4* cells was intermediate between that in Δ*sit4* cells and that in Δ*siw14* cells both in the absence and presence of caffeine (Fig. 6D, lane 3, arrow a–c versus lane 4, arrow b–c versus lane 5, arrow c; lane 9 arrow a versus lane 10, arrow b–c versus lane 11, arrow d), suggesting that Siw14 functions on phosphorylation of Gln3 independently of Sit4 and

that the function of the other factor(s) responsible for the decrease in phosphorylation level of Gln3-Myc[13] caused by Δ*siw14* disruption is negatively regulated by *SIW14*. This hypothesis was also supported by the observation that phosphorylation of Npr1-Myc[13], another target of Sit4 phosphatase activity (Jacinto et al. 2001), was not affected by the disruption of *SIW14*, indicating that Siw14 does not regulate Sit4 phosphatase activity, since the gel mobility of Npr1-Myc[13] in Δ*siw14* and Δ*siw14*Δ*sit4* cells is similar to that in wild-type and Δ*sit4* cells, respectively (Fig. 7, lane 2 and 3; arrow b, lane 4 and 5; arrow c, lane 6 and 7; arrow a, lane 8 and 9; arrow c).

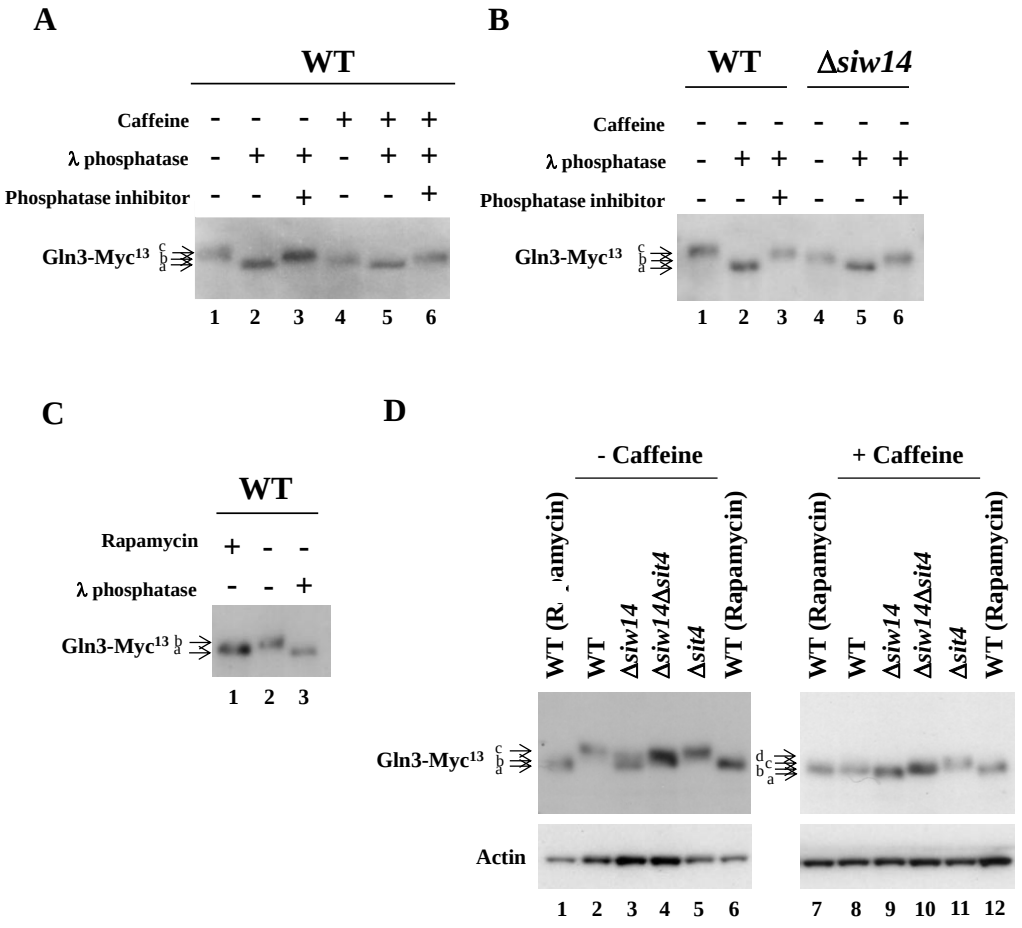

Fig. 6 Disruption of *SIT4* partially inhibits dephosphorylation of Gln3-Myc[13] in Δ*siw14* cells.
(A-C) Wild-type (MH117) and Δ*siw14* (MH118) cells were grown to mid-log phase (OD_{660} = 0.5)

in YPDA medium, and then incubated in YPDA medium containing 5 mM caffeine for 10 min or YPDA medium containing 200 ng/ml of rapamycin for 30 min. Phosphatase treatment was performed as described in 'Materials and methods' section. Gln3-Myc^{13} was detected by immunoblotting using mAB 9E10 (anti c-Myc antibody). (D) Wild-type (MH117), Δ*siw14* (MH118), Δ*sit4* (MN42), and Δ*siw14*Δ*sit4* (MN45) cells were grown to mid-log phase (OD_{660} = 0.5) in YPDA medium, and then incubated in YPDA medium containing 5 mM caffeine for 10 min or YPDA medium containing 200 ng/ml of rapamycin for 30 min. Gln3-Myc^{13} was detected by immunoblotting using mAB 9E10 (anti c-Myc antibody). Arrows indicate the migration position of phosphorylated and dephosphorylated isoforms of Gln3-Myc^{13}. Actin was used as a loading control.

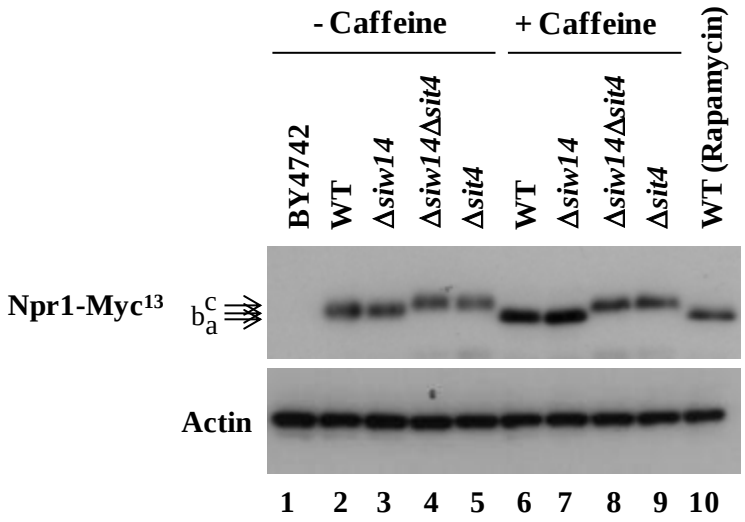

Fig. 7 Phosphorylation of Npr1-Myc^{13} is not affected by disruption of *SIW14*. B4742, wild-type (MN37), Δ*siw14* (MN74), Δ*sit4* (MN76), and Δ*siw14*Δ*sit4* (MN77) cells were grown to mid-log phase (OD_{660} = 0.5) in YPDA medium, and then incubated in YPDA medium containing 5 mM caffeine for 10 min or YPDA medium containing 200 ng/ml of rapamycin for 30 min. Npr1-Myc^{13} was detected by immunoblotting using mAB 9E10 (anti c-Myc antibody). Arrows indicate the migration position of phosphorylated and dephosphorylated isoforms of Npr1-Myc^{13}. Actin was used as a loading control.

2-3-4 Nuclear Gln3-Myc^{13} localization in response to caffeine in wild-type and Δ*siw14* cells is suppressed by the deletion of PP2A

It has been reported that Gln3 nuclear localization is also suppressed by the deletion of PP2A phosphatases, Pph21 and Pph22 (Tate et al. 2009). Therefore, I assessed the effect of deletion of PP2A phosphatases on the caffeine-induced nuclear localization of Gln3 in the Δ*siw14* cells (Fig.8). Single disruption of neither the *PPH21* gene nor the *PPH22* gene had a significant effect on the caffeine-induced nuclear localization of Gln3-Myc^{13} (Fig. 8A, C and E) because these single disruptants still retain PP2A phosphatase activity (Sneddon et al. 1990). In contrast, double disruption of both genes completely abolished the ability of Gln3-Myc^{13} to translocate to the nucleus in response to caffeine (Fig. 8G). Interestingly, the localization of Gln3-Myc^{13} in Δ*siw14*Δ*pph21* (Fig. 8D) and Δ*siw14*Δ*pph22* (Fig. 8F) cells was the same as that in Δ*pph21* (Fig. 8C) and Δ*pph22* (Fig. 8E) cells, respectively. Gln3-Myc^{13} did not show nuclear localization in response to caffeine in Δ*siw14*Δ*pph21*Δ*pph22* cells (Fig. 8G), similar to Gln3-Myc^{13} in Δ*pph21*Δ*pph22* cells (Fig. 8H). These results suggest that the increase in the caffeine-induced nuclear localization of Gln3-Myc^{13} observed in Δ*siw14* cells is due to an increase in PP2A phosphatase activity.

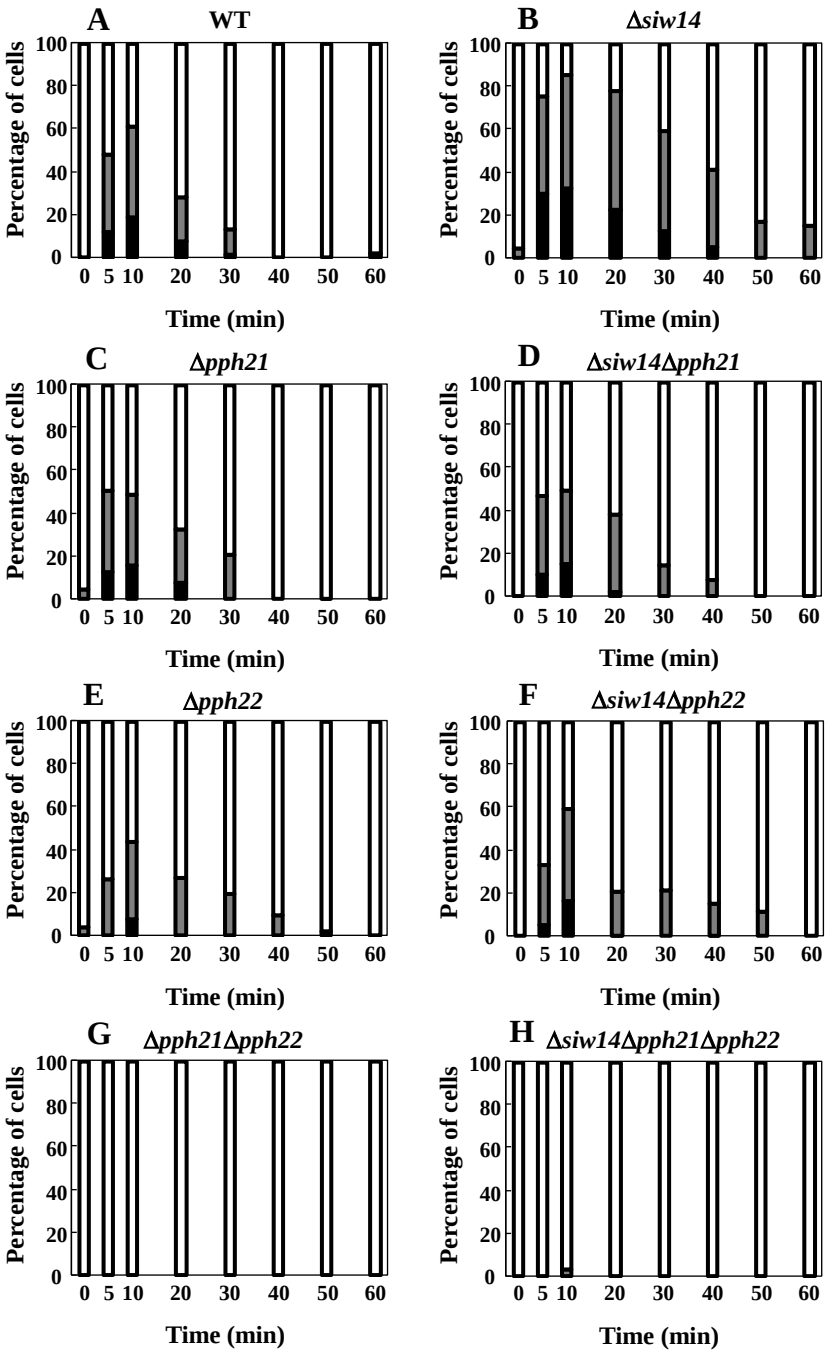

Fig. 8 The increased nuclear localization of Gln3-Myc[13] caused by disruption of *SIW14* is suppressed by a PP2A phosphatase defect. Wild-type (MH117)(A), Δ*siw14* (MH118)(B), Δ*pph21* (MN80)(C), Δ*siw14*Δ*pph21* (MN81)(D), Δ*pph22* (MN82)(E), Δ*siw14*Δ*pph22* (MN83)(F), Δ*pph21*Δ*pph22* (MN122)(G), and Δ*siw14*Δ*pph21*Δ*pph22* (MN123)(H) cells were grown to mid-log phase (OD_{660} = 0.5) in YPDA medium, and then incubated in YPDA medium containing 5 mM caffeine for 60 min. Gln3-Myc[13] localization was visualized by indirect immunofluorescence microscopy. The experimental conditions and the data presentation are the same as in Fig. 4.

2-3-5 Siw14 controls Gln3 phosphorylation through Pph21 and Pph22 phosphatases

Finally, I assessed the phosphorylation of Gln3-Myc^{13} in response to caffeine in the PP2A disruptants. In agreement with the results of Gln3-Myc^{13} localization, the change in Gln3-Myc^{13} phosphorylation in response to caffeine in Δ*pph21* or Δ*pph22* cells was similar to that in wild-type cells (Fig. 9A, lane 2, 5, and 7, arrow c; lane 10, 13, and 15, arrow b). On the other hand, Gln3-Myc^{13} showed a higher level of phosphorylation in Δ*pph21*Δ*pph22* cells than in wild-type cells in the absence of caffeine (Fig. 9B, lane 2, arrow c versus lane 5, arrow d). Under the caffeine condition, the gel mobility of Gln3-Myc^{13} in Δ*pph21*Δ*pph22* cells was intermediate between that in wild-type cells and that in Δ*sit4* cells (Fig. 9B, lane 10, arrow b versus lane 13, arrow c–d versus lane 15, arrow d). This result suggests that PP2A and Sit4 function independently in the induction of Gln3 dephosphorylation in response to caffeine.

Consistent with the alteration of Gln3-Myc^{13} localization in response to caffeine (Fig. 8), phosphorylation of Gln3-Myc^{13} in Δ*siw14*Δ*pph21* and in Δ*siw14*Δ*pph22* cells was also similar to that in wild-type cells (Fig. 9A, lane 2, 4 and 6, arrow c). Interestingly, the phosphorylation level of Gln3-Myc^{13} in Δ*siw14*Δ*pph21*Δ*pph22* cells was similar to that in Δ*pph21*Δ*pph22* cells in both the absence and presence of caffeine, suggesting that disruption of the *SIW14* gene partially decreased phosphorylation of Gln3 by increasing PP2A phosphatase activity (Fig. 9B, lane 4 and 5, arrow c–d; lane 12 and 13, arrow c–d). I also found that disruption of *TPD3*, encoding a protein which plays a role of scaffolding subunit of

PP2A complexes (van Zyl et al. 1992a), like disruption of *PPH21* and *PPH22*, suppressed decreased phosphorylation of Gln3-Myc^{13} in Δ*siw14* cells (Fig. 9C, lane 4–7; arrow b–c, and lane 12-15; arrow b–c), suggesting that decreased phosphorylation level of Gln3-Myc^{13} by disruption of *SIW14* is due to activation of Pph21–Tpd3 and Pph22–Tpd3 complexes. Taken together, these results suggest that Siw14 controls Gln3 phosphorylation by repressing Pph21–Tpd3 and Pph22–Tpd3 complexes.

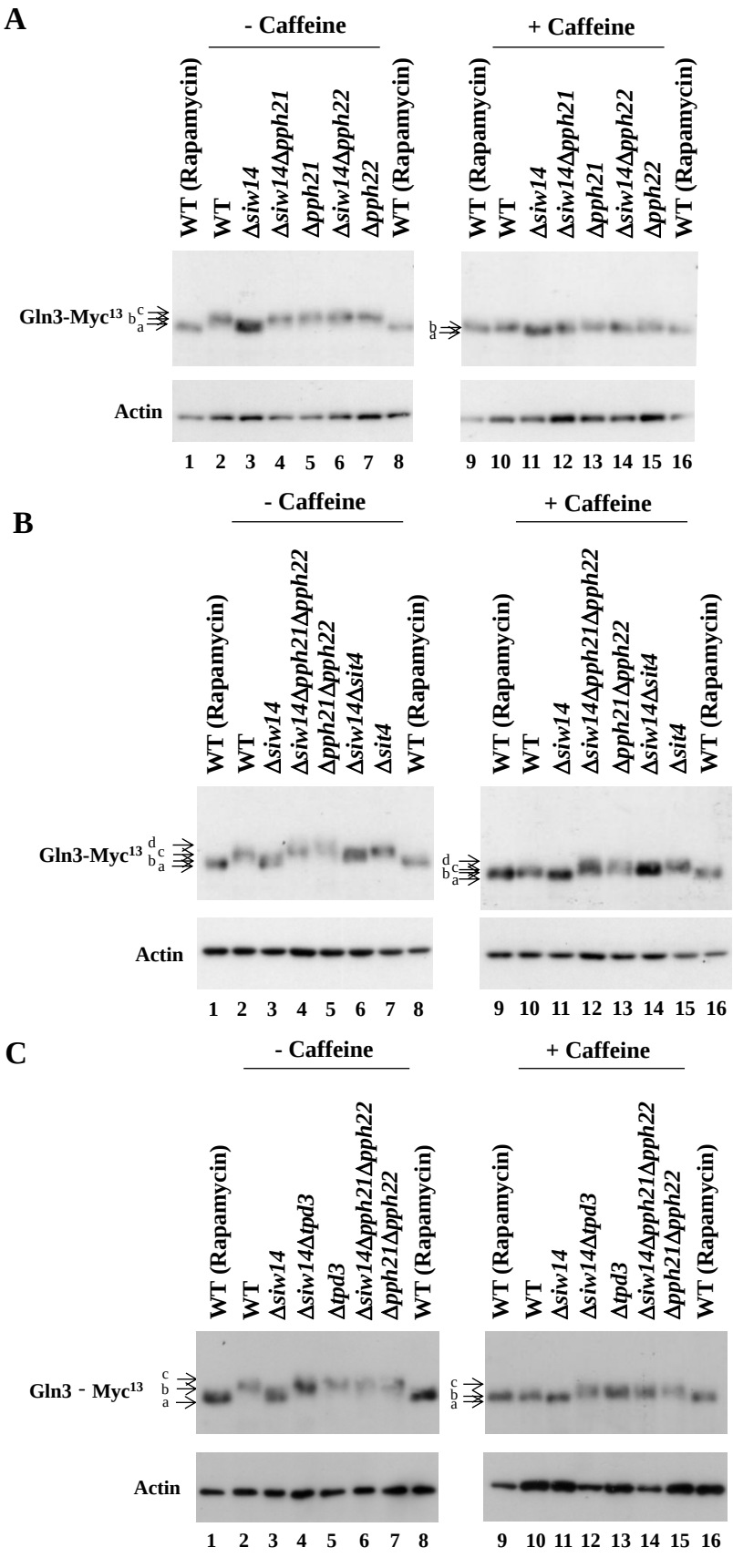
A
- Caffeine
+ Caffeine
WT (Rapamycin)
WT
Δsiw14
Δsiw14Δpph21
Δpph21
Δsiw14Δpph22
Δpph22
WT (Rapamycin)
Gln3-Myc13
Actin
1 2 3 4 5 6 7 8 9 10 11 12 13 14 15 16
B
- Caffeine
+ Caffeine
WT (Rapamycin)
WT
Δsiw14
Δsiw14Δpph21Δpph22
Δpph21Δpph22
Δsiw14Δsit4
Δsit4
WT (Rapamycin)
Gln3-Myc13
Actin
1 2 3 4 5 6 7 8 9 10 11 12 13 14 15 16
C
- Caffeine
+ Caffeine
WT (Rapamycin)
WT
Δsiw14
Δsiw14Δtpd3
Δtpd3
Δsiw14Δpph21Δpph22
Δpph21Δpph22
WT (Rapamycin)
Gln3 - Myc13
Actin
1 2 3 4 5 6 7 8 9 10 11 12 13 14 15 16

Fig. 9 Dephosphorylation of Gln3-Myc^{13} caused by disruption of *SIW14* is mediated by PP2A phosphatases. (A) Wild-type (MH117), Δ*siw14* (MH118), Δ*pph21* (MN80), Δ*siw14*Δ*pph21* (MN81), Δ*pph22* (MN82), and Δ*siw14*Δ*pph22* (MN83) cells were grown to mid-log phase (OD_{660} = 0.5) in YPDA medium, and then incubated in YPDA medium containing 5 mM caffeine for 10 min or YPDA medium containing 200 ng/ml of rapamycin for 30 min. Gln3-Myc^{13} was detected by immunoblotting using mAB 9E10 (anti c-Myc antibody). (B) Wild-type (MH117), Δ*siw14* (MH118), Δ*pph21*Δ*pph22* (MN122), Δ*siw14*Δ*pph21*Δ*pph22* (MN123), Δ*sit4* (MN42), and Δ*siw14*Δ*sit4* (MN45) cells were grown and analyzed as in panel (A). (C) Wild-type (MH117), Δ*siw14* (MH118), Δ*pph21*Δ*pph22* (MN122), Δ*siw14*Δ*pph21*Δ*pph22* (MN123), Δ*tpd3* (MN84), and Δ*siw14*Δ*tpd3* (MN85) cells were grown and analyzed as in panel (A) Arrows indicate the migration position of phosphorylated and dephosphorylated isoforms of Gln3-Myc^{13}. Actin was used as a loading control.

2-4 Discussion

It has been reported that the PP2A-like phosphatase Sit4, and the PP2A phosphatases Pph21 and Pph22 play important roles in the regulation of Gln3 localization by dephosphorylation (Tate et al. 2006, 2009). We previously discovered that the Siw14 phosphatase participates in the regulation of phosphorylation and intracellular localization of Gln3 (Hirasaki et al. 2008). However, the detailed mechanism by which Siw14 affects phosphorylation and intracellular localization of Gln3, and the relationship between Siw14 and PP2As remains still unclear. In this work, I found that Siw14 is required for negative control of the nuclear translocation and dephosphorylation of Gln3 through the repression of PP2A in response to caffeine.

We reported previously that disruption of the *SIW14* gene led to a tendency toward accumulation of Gln3 in the nucleus in the absence of caffeine (Hirasaki et al. 2008) . In the current study, however, I observed this phenotype only when caffeine was added to the medium (Fig. 4A and B). Furthermore, the temporal observation of

Gln3-Myc^{13} localization after a shift to caffeine medium indicated that disruption of *SIW14* increases the caffeine-induced nuclear localization of Gln3-Myc^{13} (Fig. 4C). These observations imply that Gln3 is unstably located in the cytoplasm in Δ*siw14* cells and readily translocates to the nucleus in response to weak caffeine stress as compared with wild-type cells. The intracellular localization of Gln3 is restricted to the cytoplasm by its interaction with Ure2, but phosphorylation of Gln3 does not affect its binding to Ure2 because both phosphorylated and dephosphorylated Gln3 can interact with Ure2 (Bertram et al. 2000). Therefore, I speculate that the low level of phosphorylated Gln3 caused by disruption of *SIW14* is able to interact with Ure2, but the complex may be unstable and more subjected to the induction of nuclear translocation in response to caffeine relative to highly phosphorylated Gln3.

Although disruption of *SIW14* has no effect on Gln3 localization in the absence of caffeine (Fig. 4A), it decreases phosphorylation of Gln3 as shown in the previous study (Hirasaki et al. 2008)(Fig. 6B and D), indicating that Siw14 indirectly controls the phosphorylation of Gln3 in the absence of caffeine. The caffeine-induced nuclear translocation of Gln3 increases dose-dependently (Fig. 4B), indicating that inhibition of TORC1 by caffeine is dose-dependent. Disruption of *SIW14* increased the caffeine-induced nuclear translocation of Gln3 (Fig. 4B and C). These results suggest that Siw14 represses nuclear translocation of Gln3 independently of TORC1 (Figure 10). I also found that deletion of the Sit4 phosphatase inhibited the caffeine-induced nuclear localization of Gln3 (Fig. 5), but only partially suppressed the decrease in phosphorylation of Gln3 (Fig. 6D, lane 3–5 and lane 9–11) in Δ*siw14* cells. On the other hand, deletion of PP2A phosphatase completely prevented both the

dephosphorylation and caffeine-induced nuclear localization of Gln3 (Figs. 8G and H, and 9B, lane 4, 5, 12, and 13). Tpd3, a scaffolding subunit of PP2A complex, was also involved in decrease of phosphorylation level of Gln3-Myc^{13} (Fig. 9C). These results suggest that Siw14 regulates the intracellular localization and phosphorylation of Gln3 mediated by PP2A–Tpd3 complexes but not Tap42–Sit4 complex (see Fig. 10). This hypothesis is also supported by the previous study showing that Sit4 and PP2A are regulated and function differently (Tate et al. 2009) and the present study indicating that Siw14 does not affect the phosphorylation of Npr1, another target of Tap42–Sit4 complex (Fig. 7). The present study also showed that caffeine induced the dephosphorylation of Gln3-Myc^{13} but did not induce nuclear translocation of Gln3-Myc^{13} in either Δ*sit4* or Δ*pph21*Δ*pph22* cells, suggesting that both Sit4 and PP2A phosphatases are required for Gln3 nuclear localization (see Fig. 10). I speculate that Ure2 interacts with Gln3 in any phosphorylation state in the absence of caffeine (see Fig. 10) since it has been reported that Ure2 binds to both phosphorylated and dephosphorylated Gln3 *in vitro* (Bertram et al. 2000). Because Ure2 is also a phosphorylated protein, which is dephosphorylated by rapamycin treatment (Hardwick et al. 1999; Cardenas et al. 1999), the interaction between Gln3 and Ure2 may require phosphorylation of Ure2 in parallel along with phosphorylation of Gln3. Once Gln3 dissociates from Ure2, however, dephosphorylated Gln3 may be preferentially imported into the nucleus. This hypothesis is supported by the present finding that dephosphorylation of Gln3 caused by disruption of *SIW14* increased the caffeine-induced nuclear localization of Gln3 (Figs. 4 and 6).

In this study, I identified a link between Siw14 and PP2A phosphatases as a

novel genetic interaction of protein phosphatases. In addition, I also found functional redundancy between Pph21 and Pph22 concerning the caffeine response of Gln3. PP2A functions in various cellular processes, including mitotic progress (Lin and Arndt 1995), cytokinesis (Lin and Arndt 1995; Healy et al. 1991), and the cell cycle checkpoint (Wang and Burke 1997; Koren et al. 2004), in addition to the TORC1 pathway (Di Como and Arndt 1996). Siw14 may act to provide the specificity of PP2A functions. Taken together, the present results provide insight into the important physiological role of Siw14 in response to caffeine.

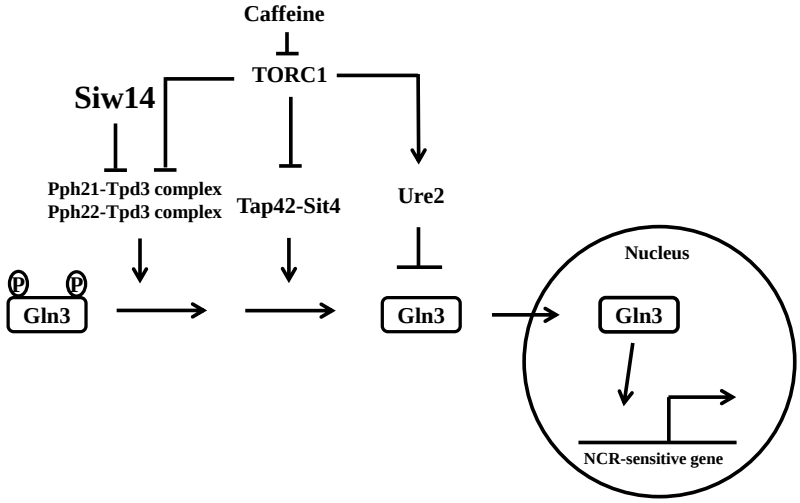

Fig. 10 Proposed model of the mechanism by which three phosphatases regulate phosphorylation and nuclear localization of Gln3. Siw14 negatively regulates Gln3 phosphorylation through the repression of PP2A phosphatases. Dephosphorylation of Gln3 by Sit4 is independent of Siw14, but dependent on the TORC1 pathway. In the absence of caffeine, Gln3 binds to Ure2, and thereby is localized in the cytoplasm. Caffeine induces both the dephosphorylation of Gln3 and Ure2 via Sit4 and/or PP2A, and the dissociation of Gln3 and Ure2. Once dissociated from Ure2, Gln3 is imported into the nucleus.

2-5 Summary

The *Saccharomyces cerevisiae* Siw14, a tyrosine phosphatase involved in the response to caffeine, participates in regulation of the phosphorylation and intracellular localization of Gln3, a GATA transcriptional activator of Nitrogen Catabolite Repression (NCR)-sensitive genes. However, the mechanism by which Siw14 controls the localization and function of Gln3 remains unclear. In this study, I show that disruption of the *SIT4* gene inhibited the caffeine-induced of Gln3-Myc^{13} in *siw14* cell. However, the decrease in phosphorylation of Gln3-Myc^{13} due to disruption of the *SIW14* gene was only partially suppressed by disruption of the *SIT4* gene. In contrast, double disruption of both the *PPH21* and *PPH22* genes completely inhibited the caffeine-induced nuclear localization of Gln3 in Δ*siw14* cells. In agreement with the localization of Gln3, the phosphorylation level of Gln3-Myc^{13} in Δ*siw14*Δ*pph21*Δ*pph22* cells, similar to Δ*pph21*Δ*pph22* cells, was higher than that in wild-type cells. I show that the increased nuclear localization of Gln3 in response to caffeine caused by disruption of the *SIW14* gene is dependent on the Sit4 and PP2A phosphatases. These results suggest that Siw14 is required for the repression of PP2A-dependent dephosphorylation and nuclear localization of Gln3 in response to caffeine and that Sit4-dependent dephosphorylation of Gln3 occurs independently of Siw14.

Chapter 3

Nuclear localization domains of transcription activator Gln3 are required for transcription of target genes through dephosphorylation in *S. cerevisiae*

3-1 Introduction

Although caffeine treatment induces nuclear translocation and transactivation of Gln3 in parallel with dephosphorylation, the details of the mechanism by which phosphorylation/dephosphorylation regulates the nuclear translocation and transactivation of Gln3 remain unclear. One approach to further elucidation of this mechanism is through identification of the phosphorylation sites present within Gln3, which would aid understanding of how phosphorylation controls Gln3 localization and transcriptional activity. To date, it has proved difficult to identify these specific phosphorylation sites because (i) the number of Gln3 molecules in the cell is very low and over-expression of Gln3 is lethal (Blinder et al. 1996; Ghaemmaghami et al. 2003); (ii) Gln3 is subject to degradation, although it is not known whether this is a physiological or artificial degradation effect (Kulkarni et al. 2006); and (iii) the Gln3 amino acid sequence contains numerous serine, threonine and tyrosine residues (199 residues in total), which prevents a site-directed mutagenesis approach. These properties have made it difficult to identify Gln3 phosphorylation sites by direct mass spectrometry analysis.

It is known that the nuclear import factor Srp1 preferentially interacts with hypophosphorylated Gln3 over hyperphosphorylated Gln3 (Carvalho et al. 2001a),

suggesting a correlation between Gln3 dephosphorylation and its nuclear localization. Therefore, I focused on Gln3 nuclear localization signals (NLS) and nuclear export signals (NES) as these are important for nuclear import and export, respectively. Calvalho and Zheng (Carvalho & Zheng 2003) identified the 336-345 region of Gln3 as a characteristic NES that interacts with the exportin, Crm1, and also identified the 388-394 region as an NLS that interacts with Srp1 (see Fig. 11A). Additionally, Kulkarni et al. (Kulkarni et al. 2001) used a systematic truncation analysis to show that the 344-365 region is required for nuclear localization and that substitution of Ser-344, Ser-347, and Ser-355 with aspartic acid results in a significant reduction in the translocation of Gln3 to the nucleus (Fig. 11A).

In Chapter 3, I introduced mutations into these NES and NLS regions of Gln3 and investigated the effects on intracellular localization and transcriptional activity. I show that these regions are involved in the regulation of phosphorylation under condition that include a preferred nitrogen source. I also found that point mutations in the 336-345 (NES) or 344-365 (NLS-K) regions from serine and threonine residues to aspartic acid, decreased the transcriptional activity of Gln3, although these mutations had no effect on caffeine-induced nuclear localization of Gln3. These observations suggest that Thr-339, Ser-344, Ser-347, and Ser-355 residues in the NLS-K and NES regions play a role in the regulation of transcriptional activity and that Gln3 activity is likely activated by dephosphorylation of these regions.

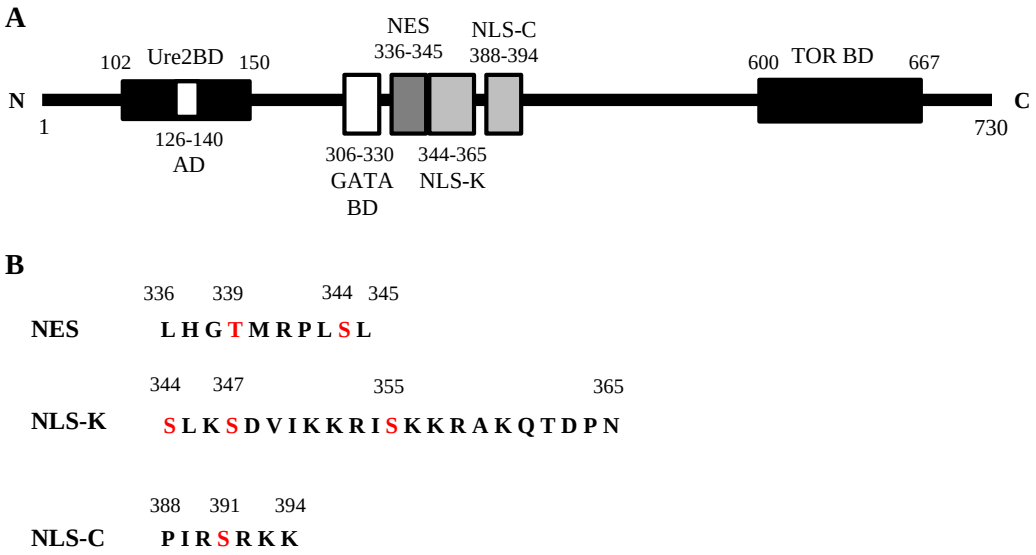

Fig. 11 Schematic representation of Gln3. (A) The structural domains of Gln3; this model is based on previous reports (Carvalho and Zheng 2003; Kulkarni et al. 2001). AD, activation domain; BD, binding domain. (B) Amino acids sequences of the NES, NLS-K and NLS-C regions (Saccharomyces Genome database; http://www.yeastgenome.org/). The residues substituted to alanine or aspartic acids are shown in red font.

3-2 Materials and methods

3-2-1 Strains and media

The yeast strains used in Chapter 3 are listed in Table 4. MH21 cells carrying *gln3* mutant plasmids (Table 5) were used for all analysis of Gln3-Myc[13]. The yeast cells were grown in standard rich medium (YPD) (Difco) containing adenine (0.04%) and SC dropout medium (Sherman 2002). The YPDA medium was supplemented with 5 mM caffeine (Wako Pure Chemical Industries) for the caffeine treatment. Yeast transformation was performed by the lithium acetate procedure (Sambrook, E.F. Fritsch 1989). All cultures were grown at 30°C. *Escherichia coli* DH5α (*supE44*, Δ*lacU169*[Φ80*lacZ*ΔM15], *hsdR17*, *recA1*, *endA1*, *gyrA96*, *thi-1*, *relA1*) was used for plasmid construction. *E.coli* strains with plasmids were grown at

37°C in LB medium (Sigma Aldrich) containing 50 μg/ml of ampicillin.

Table 4 The yeast strains used in Chapter 3

Strain	Genotype	Remarks
SH5210	*MATα ura3-52 his3Δ200 leu2Δ1 lys2Δ202 trp1Δ63*	FY834
MH117	*MATα his3Δ1 leu2Δ0 lys2Δ0 ura3Δ0 GLN3*-Myc^{13}::*CgHIS3*	(Hirasaki et al. 2008)
MH21	*MATα ura3-52 his3Δ200 leu2Δ1 lys2Δ202 trp1Δ63 Δgln3::CgHIS3*	(Hirasaki et al. 2008)

Table 5 Plasmids used in Chapter 3

Plasmid	Description
pRS316	YCp-*URA3*
pYU-WT	pRS316-*GLN3*^{WT}-Myc^{13}
pYU-ΔNES	pRS316-*GLN3*$^{\Delta 336\text{-}345}$-Myc^{13}
pYU-NES-A	pRS316-*GLN3*$^{T339A/S344A}$-Myc^{13}
pYU-NES-D	pRS316-*GLN3*$^{T339D/S344D}$ -Myc^{13}
pYU-ΔNLS-K	pRS316-*GLN3*$^{\Delta 344\text{-}365}$-Myc^{13}
pYU-NLS-K-A	pRS316-*GLN3*$^{S344A/S347A/S355A}$-Myc^{13}
pYU-NLS-K-D	pRS316-*GLN3*$^{S344D/S347D/S355D}$-Myc^{13}
pYU-ΔNLS-C	pRS316-*GLN3*$^{\Delta 388\text{-}393}$-Myc^{13}
pYU-NLS-C-A	pRS316-*GLN3*^{S391A}-Myc^{13}
pYU-NLS-C-D	pRS316-*GLN3*^{S391D}-Myc^{13}

3-2-2 Plasmid construction

The plasmids and primers used in Chpater 3 are listed in Table 5 and Table 6, respectively. The promoter and open reading frame (ORF) of the *GLN3* gene was amplified using chromosomal DNA from the SH5210 strain as the template and GLN3-1000-SalIF and GLN3-1000-NheIR, and GLN3-NheIF and GLN3-SalR as the primers, respectively. Myc^{13} was amplified using chromosomal DNA from the

MH117 strains as the template and 13Myc-SalF and 13Myc+6-HindIII as the primers. For construction of the pYU-WT plasmid, amplified fragments of the *GLN3* promoter (-1000~-1), *GLN3* ORF, and Myc[13] were inserted into the *Xho*I/*Nhe*I, *Nhe*I/*Sal*I, and *Sal*I/*Hin*dIII sites of pRS316 (Sikorski and Hieter 1989), respectively. Site-directed mutagenesis was performed using the PrimeSTAR® mutagenesis basal kit (Takara Bio, Inc.) with pYU-WT plasmids as the template and the specific primer pairs listed in Table 6. *GLN3* ORFs cloned in all plasmids were confirmed by DNA sequence analysis.

3-2-3 Immunoblotting, immunoprecipitation and phosphatase treatment

Cells were grown to OD_{660} = 0.5 at 30°C in YPDA medium after pre-incubated in SC medium. Then, caffeine and rapamycin treatment were performed by transferring cells to YPDA medium containing 5 mM caffeine and 200 ng/ml of rapamycin and incubated at 30°C for 10 min and 30 min, respectively. Protein extraction, phosphatase treatment and immunoblotting was performed as described in Chapter 2. Gln3-Myc[13] was detected using horseradish peroxidase (HRP)-conjugated anti mouse monoclonal IgG_1 (C-Myc 9E10 HRP: Santa Cruz) as previously described (Hirasaki et al. 2008). Actin as the loading control was detected using anti-Actin (Merck Millipore) and HRP-conjugated anti mouse monoclonal IgG_1 as secondary antibody.

3-2-4 Quantitative RT-PCR

Total RNA extracts were isolated from the yeast cells using a hot phenol

method (Spellman et al. 1998). First strand cDNA was synthesized using a QuantiTect® Reverse Transcription Kit (Qiagen). PCR was performed using 20 μl reaction mixtures on a Thermal Cycler Dice® Real Time System (Takara Bio, Inc.) with PrimeSTAR® Single MaxDNA Polymerase (Takara Bio, Inc.). *ACT1* was used as the internal standard to estimate relative mRNA levels. Primers for RT-PCR used in this study are described in the previous study (Hirasaki et al. 2008).

Table 6 Primers used in Chapter 3

Primer	Primer sequence
GLN3-1000-SalIF	5'-CCCGTCGACGACTAGCAGCAAAGGCAATG-3’
GLN3-1000-NheIR	5'-GGGGCTAGCTTGTTTGTTGGTGGGGGAAA-3’
GLN3-NheIF	5'-GGGGCTAGCATGCAAGACGACCCCGAAAA-3’
GLN3-SalIR	5'-GGGGTCGACTATACCAAATTTTAACCAAT -3’
13Myc-SalIF	5'-GGGGTCGACTTAATTAACGGTGAACAAAA-3’
13Myc+6-HindIR	5'-GGGAAGCTTGGATCTGCCGGTAGAGGTGT-3’
S355A-F	5'-AGGATTGCAAAGAAGAGAGCCAAACAA-3’
S355A-R	5'-CTTCTTTGCAATCCTCTTTTTGATAAC-3’
S355D-F	5'-AGGATTGATAAGAAGAGAGCCAAACAA-3’
S355D-R	5’-CTTCTTATCAATCCTCTTTTTGATAAC-3’
S344AS347A-F	5’-TAGCATTAAAAGCAGACGTTATCAA-3’
S344AS347A-R	5’-CTGCTTTTAATGCTAATGGCCTCAT-3’
S344DS347D-F	5’-AGATTTAAAAGATGACGTTATCAAAAAGAGG-3’
S344DS347D-R	5’-TCATCTTTTAAATCTAATGGCCTCATGGTACC-3’
S391AF	5’-ATACGAGCAAGGAAAAAATCACTACAA-3’
S391AR	5’-TTTCCTTGCTCGTATGGGTTTAGCATT-3’
S391DF	5’-ATACGAGACAGGAAAAAATCACTACAA-3’
S391DR	5’- TTTCCTGTCTCGTATGGGTTTAGCATT-3’
T339AS344AF	5’-AGGCCATTAGCCTTAAAATCGGACGTTATC-3’
T339AS344AR	5’-CGATTTTAAGGCTAATGGCCTCATGGCACC-3’
T339DS344DF	5’-AGGCCATTAGACTTAAAATCGGACGTTATC-3’
T339DS344DR	5’-CGATTTTAAGTCTAATGGCCTCATGTCACC-3’

Delta344-365F	5'-AGGCCATTAAAGAAGAGAGCCAAACAA-3'
Delta344-365R	5'-TCTCTTCTTTAATGGCCTCATGGTACC-3'
Delta336-345F	5'-CAGAAAAAATCGGACGTTATCAAA-3'
Delta336-345R	5'-GTCCGATTTTTTCTGGAAAAGACCGCA-3'
Delta388-394F	5'-GCTAAATCACTACAACAAAACTCT-3'
Delta388-394R	5'-TAGTGATTTAGCATTTGTAGTGGT-3'

3-3 Results and discussion

3-3-1 Mutations of serine and threonine in NES, NLS-K or NLS-C regions of Gln3 to alanine affect phosphorylation of Gln3

Caffeine treatment induces dephosphorylation of Gln3 and its translocation to the nucleus and transcription of NCR-sensitive genes. In order to identify the Gln3 phosphorylation sites that determine intracellular localization, I focused on NLS and NES domains that are important for nuclear import and export, respectively (Fig. 11A). The 336-345 amino acid region of Gln3 has been identified as an NES domain and the 344-365 and 388-394 regions as NLS domains (shown in Fig. 11A)(Carvalho & Zheng 2003; Kulkarni et al. 2001); in this thesis, I term these latter two regions as NLS-K and NLS-C, respectively. To investigate the involvement of the NES, NLS-K, and NLS-C regions in the regulation of phosphorylation, I constructed low-copy number plasmids expressing either Myc-tagged wild-type Gln3 (pYU-WT) or Gln3 carrying mutations that altered the serine and threonine residues to the non-phosphorylatable residue alanine (pYU-NES-A, pYU-NLS-K-A, and pYU-NLS-C-A). I also constructed plasmids expressing mutant *gln3* in which the NES or NLS region was completely removed (pYU-ΔNES, pYU-ΔNLS-K, and pYU-ΔNLS-C). The plasmids were introduced into Δ*gln3* cells (MH21), and phosphorylation levels were determined by

immunoblotting. I found that the gel mobility of plasmid-borne Gln3^{WT}-Myc^{13} increased after treatment with caffeine or rapamycin (Fig. 12A lane 4 and 5); a similar outcome was obtained for chromosome-bone Gln3-Myc^{13} (Fig. 6A and C). As the gel mobility of Gln3^{WT}-Myc^{13} immunoprecipitates increased after lambda protein phosphatase treatment (Fig. 12A lanes 1-3), I suggest that the increased mobility was the result of a change in the phosphorylation level. The gel mobility of Gln3-Myc^{13} treated with rapamycin was identical to that of Gln3-Myc^{13} after lambda protein phosphatase treatment. Therefore, I used Gln3-Myc^{13} treated with rapamycin as the control for the dephosphorylated form of Gln3-Myc^{13} in subsequent experiments.

With regard to the NES region, deletion of amino acids 336-345 (Gln3$^{\Delta NES}$) had no effect on gel mobility in the absence of caffeine or after lambda protein phosphatase treatment (Fig. 12B lanes 2 and 3). I suspect that the small difference in molecular weights between Gln3^{WT} and Gln3$^{\Delta NES}$ did not cause any difference in mobility under my experimental conditions; Gln3 has 729 amino acids and the deletion in the NES region resulted in the loss of 10 amino acids (Fig. 12C). In contrast to Gln3$^{\Delta NES}$, mutation of the serine and threonine residues to alanine (Gln3^{NES-A}) slightly increased gel mobility relative to Gln3^{WT} (Fig. 12B lane 4). Immunoprecipitates of Gln3^{WT}, Gln3$^{\Delta NES}$ and Gln3^{NES-A} treated with lambda protein phosphatase all exhibited the same gel mobility (Fig. 12C), indicating that the increase in gel mobility by mutation of Thr-339 and Ser-344 to alanine was caused by the decrease in phosphorylation level of Gln3-Myc^{13}. Therefore, I suggest that Thr-339 and/or Ser-344 affect the phosphorylation level of Gln3 in the presence of preferred nitrogen sources. Although I could not definitively establish the cause of

the difference in gel mobility of Gln3$^{\Delta NES}$-Myc^{13} and Gln3^{NES-A}-Myc^{13}, one possibility is that deletion of the NES region may prevent dephosphorylation of other phosphorylated regions.

With regard to the NLS region, I found that the NLS-K deletion mutant (Gln3$^{\Delta NLS-K}$) exhibited increased gel mobility relative to Gln3^{WT} (Fig. 12D lanes 2 and 3). The triple mutant of Ser-344, Ser-347, and Ser-355 to alanine (Gln3$^{NLS-K-A}$) also showed slightly increased gel mobility compared to Gln3^{WT} in the absence of caffeine (Fig. 12D lane 4). Immunoprecipitates of Gln3^{WT}, Gln3$^{\Delta NLS-K}$ and Gln3$^{NLS-K-A}$ treated with lambda protein phosphatase all exhibited the same gel mobility (Fig. 12E), indicating that the changes in molecular weight in the deletion mutants did not alter their gel mobility. This analysis suggests that the increase in gel mobility following replacement of serine residues in the NLS-K region by alanine is due to a decrease in phosphorylation of Gln3-Myc^{13} and that the 344-365 region is involved in the regulation of the phosphorylation level in the presence of preferred nitrogen sources.

With regard to the NLS-C region (388-394), I found that the deletion mutant (Gln3$^{\Delta NLS-C}$) and the mutant with the Ser-391 to alanine change (Gln3$^{NLS-C-A}$) showed increased gel mobility compared to Gln3^{WT} (Fig. 12F, lanes 2-4). Lambda protein phosphatase-treated Gln3$^{\Delta NLS-C}$ and Gln3 $^{NLS-C-A}$ showed the same mobility as Gln3^{WT} treated with lambda protein phosphatase (Fig. 12G). This finding indicates that the increase in gel mobility in the mutants was caused by a decrease in their phosphorylation levels. Taken together, the results suggest that all three of these regions affect the phosphorylation of Gln3 in the presence of preferred nitrogen

sources.

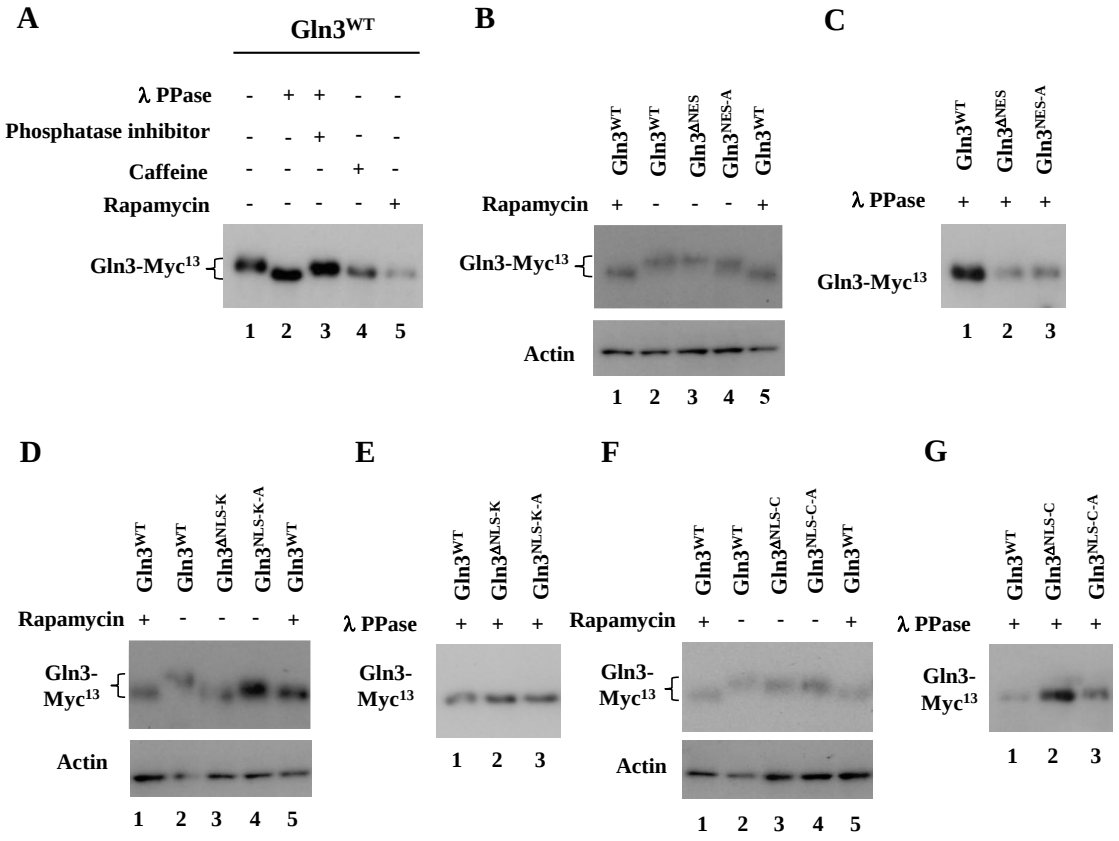

Fig. 12 Effects of NES and NLS sites on the phosphorylation level. (A) Δ*gln3* cells (MH21) carrying a pRS316 plasmid expressing Myc-tagged wild-type Gln3 (pYU-WT) were grown in YPDA medium to OD_{660} = 0.5 after pre-incubated in SC medium. Caffeine and rapamycin treatment was performed by incubating cells in YPDA medium containing 5 mM caffeine for 10 min or 200 ng/ml rapamycin for 30 min. Crude protein extraction, immunoprecipitation and phosphatase treatment (λ PPase) was performed as described in previous report (22). (B, D, F) Δ*gln3* cells (MH21) carrying each plasmid (pYU-WT, pYU-ΔNES, pYU-NES-A, pYU-ΔNLS-K, pYU-NLS-K-A, pYU-ΔNLS-C, or pYU-NLS-C-A) were grown in YPDA medium to OD_{660} = 0.5 after pre-incubated in SC medium. Δ*gln3* cells carrying pYU-WT was treated with caffeine and rapamycin treatment by incubating cells in YPDA medium containing 200 ng/ml rapamycin for 30 min. Gln3-Myc^{13} and Actin was detected by immunoblotting using mAB 9E10 (anti c-Myc antibody) and MAB1501 (Anti-Actin antibody), respectively. Actin is

used as a loading control. (C, E, G) Cells were grown as described in panel B, D, and F, respectively. Crude protein extraction, immunoprecipitation and phosphatase treatment (λ PPase) was performed as described in Chapter 2.

3-3-2 Mutation of Thr-339, Ser-344, Ser-347, Ser-355, and Ser-391 in NES, NLS-K or NLS-C regions of Gln3 to alanine or aspartic acid does not affect nuclear translocation in response to caffeine

To investigate whether phosphorylation of NES, NLS-K and NLS-C regions affected the intracellular localization of Gln3, I screened the distribution of $Gln3^{WT}$-Myc^{13} over a period of 60 min after a shift to medium containing caffeine (Fig. 13). As described in the Materials and Methods, the location of Gln3-Myc^{13} was assessed as cytoplasmic, partially nuclear, or nuclear. Before caffeine treatment (0 min), most cells carrying $Gln3^{WT}$ exhibited cytoplasmic localization (Fig. 13A); at 10 min after transfer to medium containing caffeine, ~50% of cells carrying $Gln3^{WT}$ showed nuclear or partially nuclear location of Gln3-Myc^{13} (Fig. 13A and B). Subsequently, the proportions of cells with nuclear or partially nuclear localization of $Gln3^{WT}$ decreased gradually and, within 60 min, all cells displayed only cytoplasmic localization (Fig. 13A and B). Thus, the effect of caffeine on nuclear translocation of Gln3 was transient. I suggest that this apparent transience may be due to the use here of a lower concentration of caffeine than in the previous study (Hirasaki et al. 2008).

Next, I investigated whether deletion of NES, NLS-K, or NLS-C regions affects the intracellular localization of Gln3 in response to caffeine. As expected, deletion of NES ($Gln3^{\Delta NES}$) caused increased nuclear localization in the absence of caffeine (Fig. 13C); the cells continued to show nuclear localization after transfer to medium containing caffeine (Fig. 13C). These findings are consistent with a previous

report (Carvalho and Zheng 2003) and indicate that the 336-345 region acts as a nuclear export signal. By contrast, deletion of the 344-365 NLS-K region ($Gln3^{\Delta NLS-K}$) had no effect on caffeine-induced nuclear localization of Gln3 compared to $Gln3^{WT}$ (Fig. 13B and D). Although a systematic truncation analysis previously showed that the NLS-K region is required for nuclear localization (Kulkarni et al. 2001), my analysis indicated that this region was not required for the nuclear translocation of Gln3 at least in response to caffeine. This conclusion is consistent with an earlier report that deletion of the 351-361 region has no effect on rapamycin-induced nuclear translocation of Gln3 (Carvalho and Zheng 2003). I also observed here that a lower proportion of cells carrying $Gln3^{\Delta NLS-C}$-Myc^{13} showed nuclear or partially nuclear localization of Gln3-Myc^{13} compared to $Gln3^{WT}$-Myc^{13} at 10 min after transfer to medium containing caffeine (Fig. 13B and E), although deletion of this region (ΔNLS-C) did not completely prevent caffeine-induced nuclear translocation of Gln3. Like $Gln3^{\Delta NLS-C}$, deletion of both NLS-K and NLS-C regions did not repress caffeine-induced nuclear translocation (data not shown). This latter observation suggests that other regions may participate in the nuclear translocation of Gln3 in response to caffeine in addition to the NLS-C region.

To investigate the role of phosphorylation of serine and threonine residues in the NES, NLS-K, and NLS-C regions in restricting Gln3 localization to the cytoplasm, I analyzed the intracellular localization of Gln3-Myc^{13} in cells with point mutations at all potential phosphor-acceptor sites to alanine ($Gln3^{NES-A}$, $Gln3^{NLS-K-A}$, and $Gln3^{NLS-C-A}$). No effect was observed on the intracellular localization of Gln3 in any mutant (Fig 13 F, G, and H). To determine whether dephosphorylation of these serine

and threonine residues was required for caffeine-induced nuclear translocation of Gln3, I constructed plasmids expressing *gln3* proteins with mutations at all potential phosphoacceptor sites to the mimic-phosphorylatable residue, aspartic acid (pYU-NES-D, pYU-NLS-K-D, and pYU-NLS-C-D). These plasmids were introduced into Δ*gln3* cells and the intracellular localization of Gln3 was analyzed. I found that the point mutations to aspartic acid had no effect on caffeine-induced nuclear translocation of Gln3 (Fig. 13I, J, and K), indicating that these residues were dispensable for the intracellular localization of Gln3. It is known that the intracellular localization of Gln3 is regulated by the interaction of Ure2 and Tor1 kinase activities (Kulkarni et al. 2001; Carvalho and Zheng 2003). Deletion of the Ure2 binding domain in the N-terminus or Tor1 binding domain in the C-terminus of Gln3 leads to the nuclear translocation of Gln3. Thus, the intracellular localization of Gln3 may be solely determined by the interaction with Ure2 and Tor1 and not by phosphorylation/dephosphorylation of the NES and NLS regions.

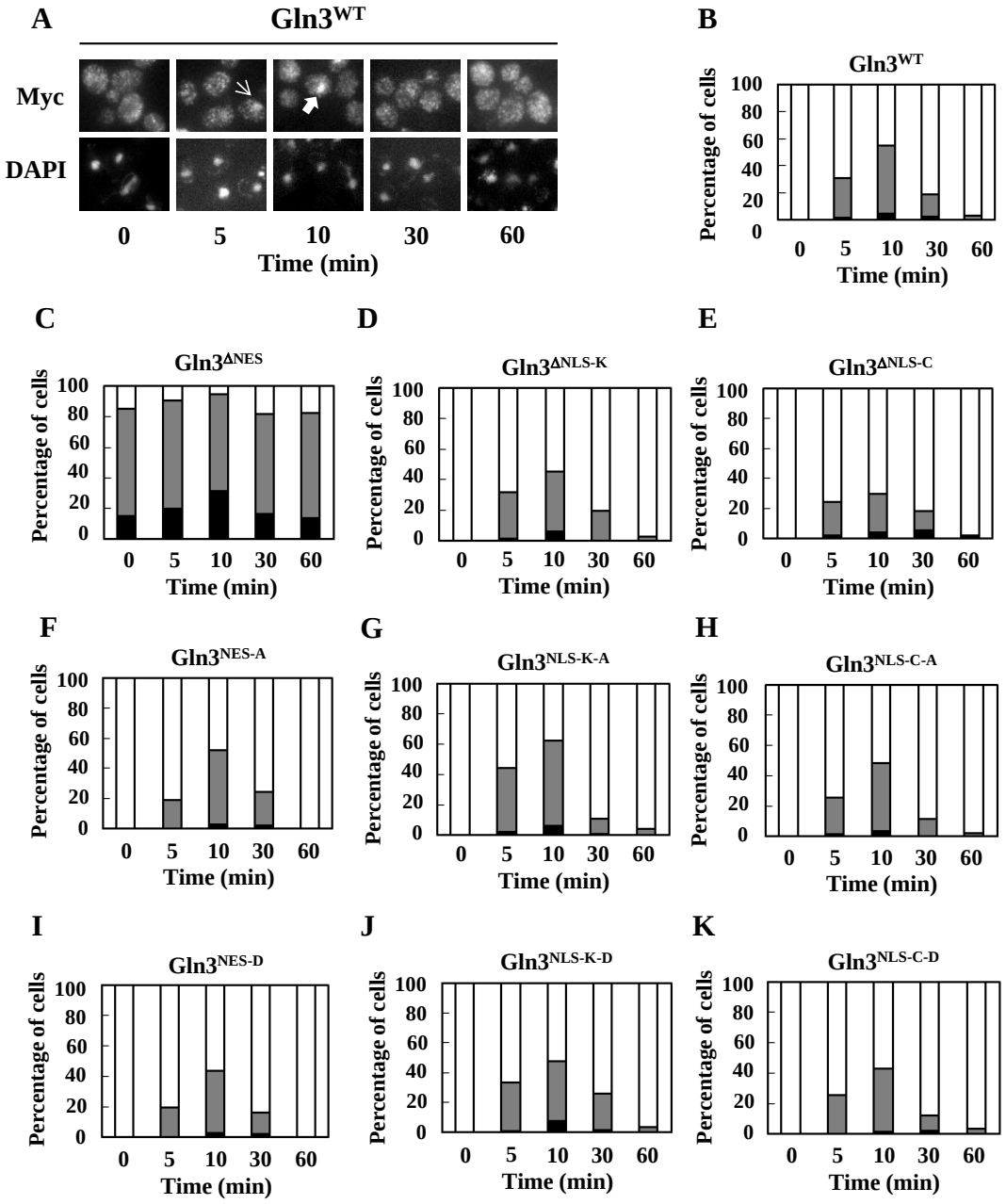

Fig. 13 Effects of mutations of NES and NLS regions on the intracellular localization in response to caffeine. Δ*gln3* cells (MH21) carrying a plasmid (pRS316, pYU-WT, pYU-ΔNES, pYU-ΔNLS-K, pYU-ΔNLS-C, pYU-NES-A, pYU-NLS-K-A, pYU-NLS-C-A, pYU-NES-D, pYU-NLS-K-D, or pYU-NLS-C-D) were grown to mid-log phase (OD_{660} = 0.5) in YPDA medium after pre-incubation in SC medium, and then incubated in YPDA medium containing 5 mM caffeine for 1h. Samples were taken at the indicated times. (A) Gln3-Myc[13] was visualized by indirect immunofluorescence microscopy. Nuclear DNA was stained with DAPI. Thick and thin arrows point to cells with nuclear localization and partial nuclear localization of Gln3, respectively.

(B-K) Gln3-Myc^{13} distribution in cells was classified as: nuclear (black), partially nuclear (gray), and cytoplasmic localization (white). Approximately 100 cells were counted, and the percentage of cells in each group is shown.

3-3-3 Mutation of Thr-339 and Ser-344 in NES or mutation of Ser-344, Ser-347, and Ser-355 in NLS-K regions of Gln3 to aspartic acid decreases caffeine-induced transcription of NCR-sensitive genes

To examine the effects of Gln3 mutations on transcriptional activity in response to caffeine, I analyzed expression of the NCR-sensitive genes, *MEP2* (which encodes an ammonium permease) and *DAL5* (which encodes an allantoate transporter) using quantitative real-time RT PCR. I found that Δ*gln3* cells expressing Gln3^{WT} showed an increase in transcription of *MEP2* and *DAL5* in response to caffeine, whereas Δ*gln3* cells carrying the control vector did not (Fig. 14). Interestingly, cells carrying Gln3$^{\Delta NES}$ did not show an induction of *MEP2* or *DAL5* transcription in the absence of caffeine (Fig. 14A), although Gln3$^{\Delta NES}$ localized to the nucleus (Fig. 13C). This suggests that other, unidentified mechanisms exist in the regulation of Gln3 transcriptional activity in addition to nuclear translocation. The levels of *MEP2* and *DAL5* transcription in cells carrying Gln3^{NES-A} exposed to caffeine were similar to those of cells carrying Gln3^{WT}. By contrast, transcription of *MEP2* and *DAL5* was not induced even by the addition of caffeine in cells carrying Gln3^{NES-D} (Fig. 14A) although Gln3^{NES-D} is localized in nucleus by caffeine treatment (Fig. 13I), suggesting that non-phosphorylation of Thr-339 and Ser-344 was required for the transcriptional activity of Gln3.

I found that the transcription of NCR-sensitive genes in Gln3$^{\Delta NLS-K}$ mutants was not induced in response to caffeine (Fig. 14B), indicating that this region is

required for transcriptional activity of Gln3. Cells carrying $Gln3^{NLS\text{-}K\text{-}A}$ exhibited a ~60% reduction and cells expressing $Gln3^{NLS\text{-}K\text{-}D}$ an ~80% reduction in caffeine-induced transcription of *MEP2* and *DAL5* compared to cells carrying $Gln3^{WT}$ (Fig. 14B). This indicates that the NLS-K region is important for transactivation of Gln3, and suggests that Ser-344, Ser-347, and Ser-355 may repress transcriptional activity of Gln3 through phosphorylation. I also analyzed the expression of *MEP2* and *DAL5* in cells carrying either ΔNES/NLS-K-A or ΔNES/NLS-K-D mutant of Gln3. Unexpectedly, transcription of *MEP2* and *DAL5* was not induced both in the absence and presence of caffeine (data not shown). Because the NES (336-345) region in part overlapped with the NLS-K (344-365) region, I assume that the absence of NES region in NLS-K-A or NLS-K-D mutant causes loss of transcriptional activity.

I also investigated the transcriptional activity in cells carrying mutations of the NLS-C region. Interestingly, deletion of the 388-394 region had no effect on transcriptional activity compared with intact Gln3 (Fig. 14C) although cells carrying $Gln3^{\Delta NLS\text{-}C}$ exhibited a slight decrease in nuclear localization in the presence of caffeine (Fig. 13E). Cells carrying $Gln3^{NLS\text{-}C\text{-}D}$ appears to show increased level in the transcription of *MEP2* and *DAL5* in the presence of caffeine (Fig. 14C). However, I suppose that phosphorylation in NLS-C region is not required for the transactivation of Gln3 since cells carrying $Gln3^{NLS\text{-}C\text{-}A}$ did not decrease the transcription of *MEP2* and *DAL5* in the presence of caffeine (Fig. 14C).

To date, it was believed that phosphorylation of Gln3 regulated its intracellular localization but did not regulate its transcriptional activity. However, my findings here show that the serine and threonine residues in the NES and NLS-K

regions plays a role in the regulation of Gln3-mediated transcriptional activity presumably through dephosphorylation rather than the intracellular localization of Gln3. Gln3$^{\Delta NES}$-Myc^{13} did not induce transcription of the NCR-sensitive genes *MEP2* and *DAL5* in the absence of caffeine despite its nuclear localization (Fig. 13C and Fig. 14A). I also found that Gln3$^{\Delta NLS\text{-}K}$-Myc^{13}, Gln3$^{NES\text{-}D}$-Myc^{13} and Gln3$^{NLS\text{-}K\text{-}D}$-Myc^{13} did not induce transcription of *MEP2* and *DAL5* although these mutant form of Gln3 were translocated into nucleus in response to caffeine (Fig. 13D, I and J, and Fig. 14B). My data suggests that the ability of Gln3 to induce transcription was regulated independently of nuclear translocation. This conclusion is consistent with a previous report that nuclear localization of Gln3 is insufficient for its recruitment to the *DAL5* promoter (Georis et al. 2008). Georis et al. (2011) also demonstrated that PP2A phosphatases Pph21 and Pph22 are required for Gln3 binding to the *DAL5* promoter although the target sites of Pph21 and Pph22 were not identified. Further studies will be needed to confirm whether dephosphorylation of the NLS-K and NES regions in Gln3 is required for binding to the promoters of target genes. In conclusion, the Thr-339, Ser-344, Ser-347, and Ser-355 within nuclear localization domains (NES and NLS-K) in Gln3 is involved in the regulation of transcription of target genes likely via dephosphorylation in response to caffeine, and presumably to other nutrient stresses.

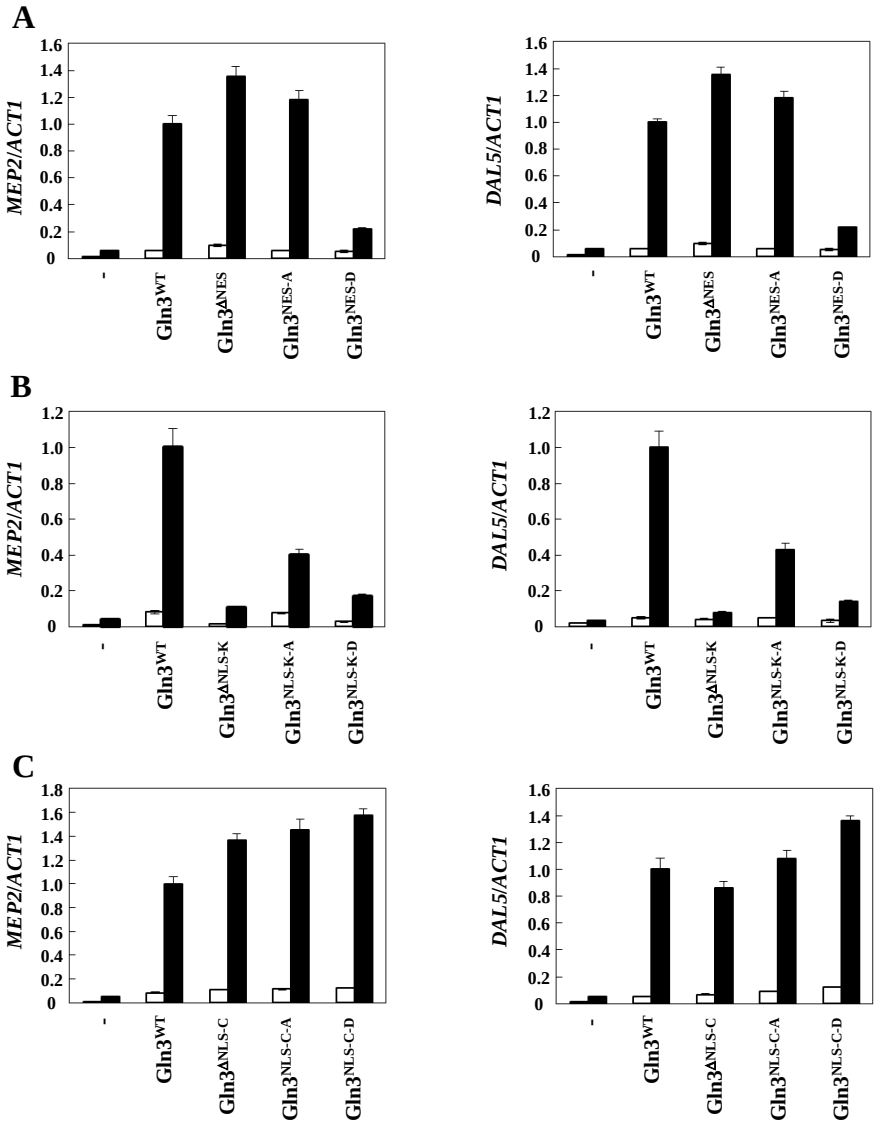

Fig. 14 Effects of mutations of NES and NLS regions on the transcriptional activity of Gln3. (A-C) Total RNA was isolated from cells grown as described in Fig. 3, and incubated in YPDA medium containing 5 mM caffeine for 30 min. mRNA levels were quantified by quantitative real time PCR as described in the 'Materials and methods' section. The relative mRNA levels of *MEP2* and *DAL5* are normalized against that of *ACT1*. The mRNA levels of *MEP2* and *DAL5* in cells carrying $Gln3^{WT}$ grown in medium containing caffeine are defined as 1.0. The white bar indicates the mRNA level of each gene before the shift to caffeine-containing YPDA medium, while the black bar indicates the level after transfer.

3-4 Summary

In this chapter, I focused on two regions of Gln3 with Nuclear Localization Signal properties (NLS-K, and NLS-C) and one with Nuclear Export Signal activity (NES). I constructed various mutants for the identification of amino acid residues which regulates the intracellular localization and transcriptional activity of Gln3 by phosphorylation/dephosphorylation: *gln3* containing point mutations in all potential phosphoacceptor sites, Thr-339 and Ser-344 in NES regions, Ser-344, Ser-347, and Ser-355 in NLS-K region, and Ser-391 in NLS-C region to produce non-phosphorylatable (alanine) or mimic-phosphorylatable (aspartic acid) residues, and deletion mutants of NLS and NES regions. I found that all of these mutations to alanine decreased phosphorylation level of Gln3 and that the aspartic acid substitution mutants showed drastic reduction of Gln3-mediated transcriptional activity despite the fact that the mutations had no effect on nuclear localization of Gln3. These observations suggest that these regions of Gln3 are required for transcription of target genes presumably through dephosphorylation.

Chapter 4
General discussion and conclusion

Activity of transcription factors is often regulated by phosphorylation/dephosphorylation (Gardner and Montminy 2005). A GATA-type transcription activator Gln3 is dephosphorylated by caffeine treatment, and leads to the nuclear translocation and expression of NCR-sensitive genes. We found in our previous study (Hirasaki et al. 2008) that disruption of *SIW14* causes the increase in the caffeine-induced nuclear translocation and the decreased phosphorylation level of Gln3. However, the detailed mechanism by which Siw14 controls the intracellular localization and function of Gln3 remains unclear. In this study, I aimed to understand the mechanism by which Siw14 regulates the phosphorylation/dephosphorylation, intracellular localization and transcriptional activity of Gln3.

It has been known that the dephosphorylation and nuclear translocation of Gln3 by caffeine treatment are induced by PP2A phosphatases Pph21/Pph22 and PP2A like phosphatase Sit4 (Tate et al. 2006, 2009). In Chapter 2, I initially examined the relation between Siw14 and Sit4 in the regulation of Gln3 localization and phosphorylation. Disruption of *SIT4* suppressed the caffeine-induced nuclear translocation of Gln3 in Δ*siw14* cells (Fig. 5). However, unexpectedly, the decreased phosphorylation level of Gln3 in Δ*siw14* cells was not completely suppressed by disruption of *SIT4* (Fig. 6D). This data suggests that Siw14 may control phosphorylation of Gln3 independently of Sit4–Tap42 complex. This hypothesis was

supported by the data that Siw14 does not affect the phosphorylation of Npr1, another well known target of Tap42–Sit4 complex (Fig. 7) (Jacinto et al. 2001). On the other hand, disruption of Pph21/Pph22 completely prevented both the dephosphorylation and caffeine-induced nuclear localization of Gln3 in Δ*siw14* cells (Fig. 8 and Fig. 9B). Pph21/Pph22 exhibits phosphatase activity by forming the Pph21/Pph22–Tap42 complex (Fig. 3C) (Di Como and Arndt 1996; Wang et al. 2003) or Pph21/Pph22–Tpd3 complex (Fig. 3A) (Ronne et al. 1991; van Zyl et al. 1992b; Shu et al. 1997). Disruption of *TPD3*, like disruption of *PPH21*/*PPH22*, suppressed the decrease of phosphorylation in Δ*siw14* cells (Fig. 9C), suggesting that Siw14 controls the intracellular localization and phosphorylation of Gln3 mediated by PPh21/Pph22–Tpd3 complex but not Tap42–Sit4 complex. Pph21/Pph22 is also required for activation of glycogen synthase encoded by *GSY1* and *GSY2* which are expressed via inhibition of TORC1 (Clotet et al. 1995; Unnikrishnan et al. 2003). I observed that disruption of *SIW14* increased caffeine-induced glycogen accumulation and that its increased glycogen accumulation was suppressed by disruption of both *PPH21* and *PPH22* but not *SIT4* (data not shown). This result supports a possibility that disruption of *SIW14* increases the activity of Pph21/Pph22–Tpd3 complex in response to caffeine, although it remains to be clarified whether Siw14 directly controls Pph21/Pph22 activity or not.

Furthermore, in Chapter 3, I attempted to identify the phosphorylation sites which regulate the intracellular localization and transcriptional activity of Gln3. Here, I focused on the NLS and NES regions, because the phosphorylation of NLS region in transcription factors often regulates the nuclear localization (Gardner and Montminy

2005). For example, *S. cerevisiae* transcription activator Swi5 is localized in nucleus by dephosphorylation and activates transcription of genes expressed at the M/G1 phase boundary and in G1 phase (Nasmyth et al. 1990). Moll et al. (1991) reported that the mutation of serine residues (Ser-522, Ser-646, and Ser-664) in NLS of Swi5 to alanine results in constitutive nuclear entry. However, the mutations of serine and threonine residues to alanine or aspartic acid in all NES, NLS-K and NLS-C regions of Gln3 have no effect on the intracellular localization of Gln3 in response to caffeine (Fig. 13). These results suggest the existence of other regions that regulate the intracellular localization of Gln3. It is known that the intracellular localization of Gln3 is regulated by the interaction of Ure2 and Tor1 kinase activities (Beck and Hall 1999; Bertram et al. 2000). Deletion of the Ure2 binding domain in the N-terminus or Tor1 binding domain in the C-terminus of Gln3 results in constitutive nuclear localization (Carvalho and Zheng 2003; Kulkarni et al. 2001). Gln3 in Δ*ure2* cells also shows constitutive nuclear localization (Beck and Hall 1999). Therefore, the intracellular localization of Gln3 may be solely determined by the interaction with Ure2 and Tor1 and not by phosphorylation/dephosphorylation of the NES and NLS regions. As described in Chapter 2, Sit4 and Pph21/Pph22 induce the nuclear translocation of Gln3 through dephosphorylation in response to caffeine. Therefore, I speculate that these phosphatases may target other phosphorylation sites than those in NES and NLS regions and regulate the interaction between Gln3 and Ure2 in cytoplasm.

On the other hand, I found that the mutations of serine and threonine residues to aspartic acid in NES and NLS-K regions prevent transcription of Gln3-target genes *MEP2* and *DAL5* in the presence of caffeine (Fig. 14A and B), suggesting that

dephosphorylation of NES and NLS-K regions is required for transcription of *MEP2* and *DAL5* in response to caffeine. NES-deleted Gln3 mutant activated the transcription of *MEP2* and *DAL5* only in the presence of caffeine (Fig. 13A) but not in the absence of caffeine although $Gln3^{\Delta NES}$ exhibited constitutive nuclear localization (Fig. 13C). I also found that $Gln3^{NES\text{-}D}$ and $Gln3^{NLS\text{-}K\text{-}D}$ did not induce the transcription of *MEP2* and *DAL5* in response to caffeine despite that they display the nuclear localization (Fig. 14A). These findings suggest that the dephosphorylation of Gln3 is required for transcription of target genes after the nuclear translocation. Georis et al. (2011) demonstrated that Pph21/Pph22 are required for Gln3 binding to the *DAL5* promoter. Therefore, it was speculated that dephosphorylation of NES and NLS-K regions may be required for binding to the promoter of Gln3-targeted genes.

Based on this study, I propose following model for the regulation of Gln3 localization and transcriptional activity by Siw14, Sit4, and Pph21/Pph22 as shown in Fig. 15. In the absence of caffeine, phosphorylated Gln3 localizes in cytoplasm with binding to Ure2. Under this condition, it is suggested from the result in Chapter 2 that Sit4–Tap42 complex is inhibited by TORC1, whereas Pph21/Pph22–Tpd3 complex is inhibited by Siw14 (see Fig. 15). I assume that caffeine activates both Sit4 and Pph21/Pph22 and induces the dephosphorylaiton at presumably different sites in Gln3. I found that dephosphorylation of Gln3 by these phosphatases leads to nuclear translocation. However, I also found from the result in Chapter 3 (Fig. 14A and B) that dephosphorylation of NES and NLS-K regions in Gln3 is required for the transcription of targeted genes in response to caffeine in addition to the dephosphorylation for nuclear translocation. Georis et al. (2011) demonstrated that

Pph21/Pph22 but not Sit4 are required for Gln3 binding to the *DAL5* promoter. Therefore, I propose that Pph21/Pph22 dephosphorylate the phosphorylated serine and threonine residues in these regions for the binding to the promoter of target genes. This idea is consistent with the result of previous report that disruption of *SIW14* increased the transcription of Gln3-targeted genes in response to caffeine (Hirasaki et al. 2008) because I found from the result in Chapter 2 that Siw14 acts upstream of *PPH21*/*PPH22* (Fig. 15). However, the phosphorylation sites which regulate the intracellular localization of Gln3 and are targeted by Sit4 and Pph21/Pph22 are not identified yet. Further studies will be needed to identify the phosphorylation sites targeted by Sit4 and Pph21/Pph22 and to confirm whether dephosphorylation of the NLS-K and NES regions in Gln3 is required for binding to the promoters of target genes. These studies will facilitate to understanding of the detailed mechanism by which the intracellular localization and transcriptional activity of Gln3 are regulated by dephosphorylation.

Cells showed nuclear localization of Gln3 at 10 min after the shift to medium containing a low concentration of caffeine and subsequently the amount of Gln3 present in nucleus decreased (Fig. 4C). The time when transcription factors localize in the nucleus are regulated by degradation or by nuclear exclusion and these processes are often regulated by phosphorylation/dephosphorylation (Whitmarsh and Davis 2000). Because Gln3 has NES region in 336-345 regions and deletion of this region or the temperature-sensitive mutation of *CRM1*, a known exporting factor, causes constitutive nuclear translocation, it was suggested that Gln3 is excluded from nucleus by Crm1 but not degraded in nucleus (Fig. 13C) (Carvalho et al. 2001b; Carvalho and

Zheng 2003). However, in this study the mutation of serine and threonine residues in NES region to alanine or aspartic acid had no effect on the intracellular localization of Gln3 in response to caffeine (Fig. 13F and I), suggesting that phosphorylation in NES region is not required for the interaction with Crm1. In Chapter 2, I found that ~60% of wild-type cells displayed the nuclear localization of Gln3 at 10 min after shift to the caffeine medium and subsequently the cells that displayed nuclear localization of Gln3 gradually decreased (Fig.4C). At 40 min after shift to the caffeine medium, nearly all cells displayed only cytoplasmic localization of Gln3 (Fig. 4C). On the other hand, more than 80% of Δ*siw14* cells showed nuclear localization of Gln3 within 5 min and this distribution remained until 20 min (Fig. 4C). However, like wild-type cells, Δ*siw14* cells that showed nuclear localization of Gln3 subsequently decreased, and at 60 min after the shift to caffeine medium, more than 90% of cells displayed cytoplasmic localization of Gln3 (Fig. 4C). Since disruption of *SIW14* promotes the nuclear translocation of Gln3 in response to caffeine but not affects export of Gln3 from nucleus, I suggest that Siw14 acts for repression of nuclear translocation of Gln3 rather than nuclear exclusion.

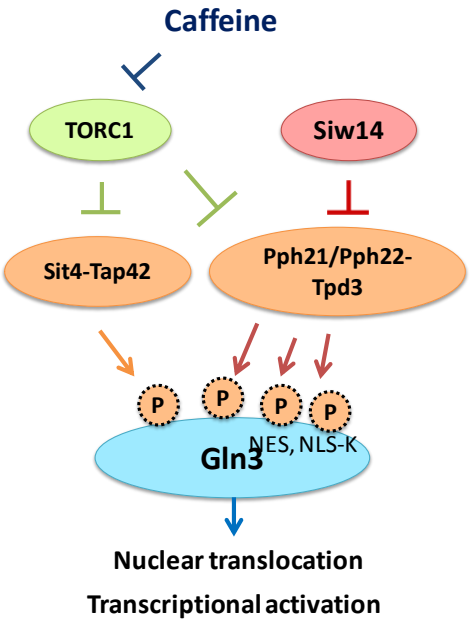

Fig. 15 The new model for the regulation of Gln3 localization and transcription activity by Siw14, Sit4 and Pph21/Pph22.

Our goal in protein phosphatase study is to define the roles of individual protein phosphates in cell physiology and to uncover the entire regulatory network of protein phosphatases in *S. cerevisiae*. Toward this goal, we started this project by constructing 30 single disruptants and 435 double disruptants of protein phosphatases in all possible combinations at that time (Sakumoto et al. 1999, 2002), and very recently 127 multiple disruptants in all possible combinations in PP2C phosphatases (Sharmin et al. 2014). Systematic phenotypic analysis of these disruptants revealed the novel genetic interactions among protein phosphatases. For example, the disruption of both *MSG5* encoding a dual-specific protein phosphatase, and *PTP2* encoding a tyrosine phosphatase, leads to calcium sensitivity (Hermansyah et al. 2009, 2010; Laviña et al. 2013a, 2013b). It was also found that the quadruple disruption of *PTC2*, *PTC3*, *PTC5* and *PTC7* increased high-temperature sensitivity (Sharmin et al.

2014). In this study, I identified a link between Siw14 and PP2A phosphatases as a novel genetic interaction in the regulation of Gln3 phosphorylation and localization. It is known that PP2A functions in various cellular processes, including mitotic progress (Lin and Arndt 1995), cytokinesis (Lin and Arndt 1995; Healy et al. 1991), and the cell cycle checkpoint (Wang and Burke 1997; Koren et al. 2004), in addition to the TORC1 pathway (Di Como and Arndt 1996). However, it remains to be seen whether Siw14 is involved in these cellular processes. Further study to elucidate the correlation between Siw14 and PP2A phosphatases will be important to understand the physiological function of Siw14. However, I believe that the present results provide insight into the important physiological role of protein phosphatases in the regulation of transcription factors in eukaryotes.

S. cerevisiae is one of the best characterized organisms not only as model of eukaryotic cells but also for biotechnological applications such as agriculture, industrial biotechnology, food engineering, and medical engineering. Understanding of the regulation mechanism of transcription factors is one of the important issues in bioengineering for breeding of industrial strains which must have the best expression profile for the high production efficiency and the environmental stress tolerance. For example, it was reported that *MSN4*, one of transcriptional activators for activating transcription of genes via the stress response element, are defective in sake yeast strains and expression of functional *MSN4* leads to delay of the ethanol fermentation in sake yeast, suggesting that dysfunction of *MSN4* is important for the effective ethanol fermentation during sake brewing (Watanabe et al., 2011). Gln3 activates transcription of NCR-sensitive genes such as genes encoding the amino acid

transporters and the enzymes needed for biosynthesis of amino acids in response to nitrogen sources in the environment (Cooper 2002). Amino acids are important for the determination of tasty and flavor in fermented foods and alcoholic drinks. *S. cerevisiae* can utilize a variety of nitrogen compounds as nitrogen sources and make all of $_{L}$-amino acids (Ljungdahl and Daignan-Fornier 2012). Disruption of *SIW14* increases nuclear translocation of Gln3 and transcription of NCR-sensitive genes induced by caffeine treatment (Fig. 4C) Hirasaki et al. 2008), suggesting that Siw14 is involved in the control of Gln3 transcriptional activity in response to non-preferred nitrogen sources. The analysis of the mechanism for caffeine-induced nuclear translocation of Gln3 and transcription of NCR-sensitive genes would be beneficial not only for understanding the mechanism by which the intracellular localization and transcriptional activity of Gln3 is controlled in response to non-preferred nitrogen sources, but also for the development of breeding strategy for yeast strains artificially coordinating amino acid content to determine the pleasantness of the taste and flavor in food biotechnology.

References

Alonso, A., Sasin, J., Botini, N., Friedberg, I., Friedberg, I., Osterman, A., Godzik, A., Hunter, T., Dixon, J., and Mustelin T. (2004) Protein tyrosine phosphatases in the human genome. *Cell* 117: 699–711.

Beck, T. and Hall, M. N. (1999) The TOR signalling pathway controls nuclear localization of nutrient-regulated transcription factors. *Nature* 402: 689–692.

Bertram, P. G., Choi, J. H., Carvalho, J., Ai, W., Zeng, C., Chan, T. F. and Zheng, X. F. (2000) Tripartite regulation of Gln3p by TOR, Ure2p, and phosphatases. *J. Biol. Chem.* 275: 35727–35733.

Blinder, D., Coschigano, P. W. and Magasanik, B. (1996) Interaction of the GATA factor Gln3p with the nitrogen regulator Ure2p in *Saccharomyces cerevisiae*. *J. Bacteriol.* 178: 4734–4736.

Bode, A. M. and Dong, Z. (2007) The enigmatic effects of caffeine in cell cycle and cancer. *Cancer Lett.* 247: 26–39.

Broach, J. R. (2012) Nutritional control of growth and development in yeast. *Genetics* 192: 73–105.

Cardenas, M. E., Cutler, N. S., Lorenz, M. C., Di Como, C. J. and Heitman, J. (1999) The TOR signaling cascade regulates gene expression in response to nutrients. *Genes Dev.* 13: 3271–3279.

Care, A., Vousden, K. A., Binley, K. M., Radcliffe, P., Trevethick, J., Mannazzu, I. and Sudbery, P. E. (2004) A synthetic lethal screen identifies a role for the cortical actin patch/endocytosis complex in the response to nutrient deprivation in *Saccharomyces cerevisiae*. *Genetics* 166: 707–719.

Carvalho, J., Bertram, P. G., Wente, S. R. and Zheng, X. F. (2001a) Phosphorylation regulates the interaction between Gln3p and the nuclear import factor Srp1p. *J. Biol. Chem.* 276: 25359–25365.

Carvalho, J. and Zheng, X. F. (2003) Domains of Gln3p interacting with karyopherins, Ure2p, and the target of rapamycin protein. *J. Biol. Chem.* 278: 16878–16886.

Clotet, J., Posas, F., Hu, G. Z., Ronne, H. and Ariño, J. (1995) Role of protein phosphatase 2A in the control of glycogen metabolism in yeast. *Eur. J. Biochem.* 229: 207–214.

Di Como, C. J. and Arndt, K. T. (1996) Nutrients, via the Tor proteins, stimulate the association of Tap42 with type 2A phosphatases. *Genes Dev.* 10: 1904–1916.

Conrad, M., Schothorst, J., Kankipati, H. N., Van Zeebroeck, G., Rubio-Texeira, M. and Thevelein, J. M. (2014) Nutrient sensing and signaling in the yeast *Saccharomyces cerevisiae*. *FEMS Microbiol. Rev.* 38: 254–299.

Cooper, T. G. (2002) Transmitting the signal of excess nitrogen in *Saccharomyces cerevisiae* from the Tor proteins to the GATA factors: connecting the dots. *FEMS Microbiol. Rev.* 26: 223–238.

Düvel, K., Santhanam, A., Garrett, S., Schneper, L. and Broach, J. R. (2003) Multiple roles of Tap42 in mediating rapamycin-induced transcriptional changes in yeast. *Mol. Cell* 11: 1467–1478.

Gardner, K. H. and Montminy, M. (2005) Can you hear me now? Regulating transcriptional activators by phosphorylation. *Sci. STKE* 2005: pe44.

Georis, I., Feller, A., Tate, J. J., Cooper, T. G. and Dubois, E. (2009) Nitrogen catabolite repression-sensitive transcription as a readout of Tor pathway regulation: the genetic background, reporter gene and GATA factor assayed determine the outcomes. *Genetics* 181: 861–874.

Georis, I., Tate, J. J., Cooper, T. G. and Dubois, E. (2008) Tor pathway control of the nitrogen-responsive *DAL5* gene bifurcates at the level of Gln3 and Gat1 regulation in *Saccharomyces cerevisiae*. *J. Biol. Chem.* 283: 8919–8929.

Georis, I., Tate, J. J., Feller, A., Cooper, T. G. and Dubois, E. (2011) Intranuclear function for protein phosphatase 2A: Pph21 and Pph22 are required for rapamycin-induced GATA factor binding to the *DAL5* promoter in yeast. *Mol. Cell. Biol.* 31: 92–104.

Ghaemmaghami, S., Huh, W. K., Bower, K., Howson, R. W., Belle, A., Dephoure, N., O'Shea, E. K. and Weissman, J. S. (2003) Global analysis of protein expression in yeast. *Nature* 425: 737–741.

Hampsey, M. (1997) A review of phenotypes in *Saccharomyces cerevisiae*. *Yeast* 13: 1099–1133.

Hardwick, J. S., Kuruvilla, F. G., Tong, J. K., Shamji, A. F. and Schreiber, S. L. (1999) Rapamycin-modulated transcription defines the subset of nutrient-sensitive signaling pathways directly controlled by the Tor proteins. *Proc. Natl. Acad. Sci. U. S. A.* 96: 14866–14870.

Healy, A. M., Zolnierowicz, S., Stapleton, A. E., Goebl, M., DePaoli-Roach, A. A. and Pringle, J. R. (1991) *CDC55*, a *Saccharomyces cerevisiae* gene involved in cellular morphogenesis: identification, characterization, and homology to the B subunit of mammalian type 2A protein phosphatase. *Mol. Cell. Biol.* 11: 5767–5780.

Hermansyah, Laviña, W. A., Sugiyama, M., Kaneko, Y. and Harashima, S. (2010) Identification of protein kinase disruptions as suppressors of the calcium sensitivity of S. cerevisiae Deltaptp2 Deltamsg5 protein phosphatase double disruptant. *Arch. Microbiol.* 192: 157–165.

Hermansyah, Sugiyama, M., Kaneko, Y. and Harashima, S. (2009) Yeast protein phosphatases Ptp2p and Msg5p are involved in G1-S transition, *CLN2* transcription, and vacuole morphogenesis. *Arch. Microbiol.* 191: 721–733.

Hirasaki, M., Kaneko, Y. and Harashima, S. (2008) Protein phosphatase Siw14 controls intracellular localization of Gln3 in cooperation with Npr1 kinase in *Saccharomyces cerevisiae*. *Gene* 409: 34–43.

Hofman-Bang, J. (1999) Nitrogen catabolite repression in *Saccharomyces cerevisiae*. *Mol. Biotechnol.* 12: 35–73.

Jacinto, E., Guo, B., Arndt, K. T., Schmelzle, T. and Hall, M. N. (2001) *TIP41* interacts with *TAP42* and negatively regulates the TOR signaling pathway. *Mol. Cell* 8: 1017–1026.

Koren, R., Rainis, L. and Kleinberger, T. (2004) The scaffolding A/Tpd3 subunit and high phosphatase activity are dispensable for Cdc55 function in the *Saccharomyces cerevisiae* spindle checkpoint and in cytokinesis. *J. Biol. Chem.* 279: 48598–48606.

Kulkarni, A., Buford, T. D., Rai, R. and Cooper, T. G. (2006) Differing responses of Gat1 and Gln3 phosphorylation and localization to rapamycin and methionine sulfoximine treatment in *Saccharomyces cerevisiae*. *FEMS Yeast Res.* 6: 218–229.

Kulkarni, A., Abul-Hamd, A. T., Rai, R., El Berry, H. and Cooper, T. G. (2001) Gln3p nuclear localization and interaction with Ure2p in *Saccharomyces cerevisiae*. *J. Biol. Chem.* 276: 32136–32144.

Kuranda, K., Leberre, V., Sokol, S., Palamarczyk, G. and François, J. (2006) Investigating the caffeine effects in the yeast *Saccharomyces cerevisiae* brings new insights into the connection between TOR, PKC and Ras/cAMP signalling pathways. *Mol. Microbiol.* 61: 1147–1166.

Lander, E. S., Linton, L. M., Birren, B., Nusbaum, C., Zody, M. C., Baldwin, J., Devon, K., Dewar, K., Doyle, M., FitzHugh, W. et al. (2001) Initial sequencing and analysis of the human genome. *Nature* 409: 860–921.

Laviña, W. A., Hermansyah, Sugiyama, M., Kaneko, Y. and Harashima, S. (2013) Functionally redundant protein phosphatase genes *PTP2* and *MSG5* co-regulate the calcium signaling pathway in *Saccharomyces cerevisiae* upon exposure to high extracellular calcium concentration. *J. Biosci. Bioeng.* 115: 138–146.

Laviña, W. A., Shahsavarani, H., Saidi, A., Sugiyama, M., Kaneko, Y. and Harashima, S. (2013) Suppression mechanism of the calcium sensitivity in *Saccharomyces cerevisiae ptp2*Δ*msg5*Δ double disruptant involves a novel HOG-independent function of Ssk2, transcription factor Msn2 and the protein kinase A component Bcy1. *J. Biosci. Bioeng.*117: 135-141.

Lin, F. C. and Arndt, K. T. (1995) The role of *Saccharomyces cerevisiae* type 2A phosphatase in the actin cytoskeleton and in entry into mitosis. *EMBO J.* 14: 2745–2759.

Ljungdahl, P. O. and Daignan-Fornier, B. (2012) Regulation of amino acid, nucleotide, and phosphate metabolism in *Saccharomyces cerevisiae*. *Genetics* 190: 885–929.

Luan, S. (2002) Tyrosine phosphorylation in plant cell signaling. *Proc. Natl. Acad. Sci. U. S. A.* 99: 11567–11569.

Luke, M. M., Della Seta, F., Di Como, C. J., Sugimoto, H., Kobayashi, R. and Arndt, K. T. (1996) The SAP, a new family of proteins, associate and function positively with the *SIT4* phosphatase. *Mol. Cell. Biol.* 16: 2744–2755.

Manning, G., Whyte, D. B., Martinez, R., Hunter, T. and Sudarsanam, S. (2002) The protein kinase complement of the human genome. *Science* 298: 1912–1934.

McPhersonx, P. S., Kim, Y. K., Valdivia, H., Knudson, C. M., Takekura, H., Franzini-Armstrong, C., Coronadot, R. and Campbell, K. P. (1991) The brain ryanodine receptor: A caffeine-sensitive calcium release channel. *Neuron* 7: 17–25.

Moll, T., Tebb, G., Surana, U., Robitsch, H. and Nasmyth, K. (1991) The role of phosphorylation and the *CDC28* protein kinase in cell cycle-regulated nuclear import of the *S. cerevisiae* transcription factor *SW15*. *Cell* 66: 743–758.

Nasmyth, K., Adolf, G., Lydall, D. and Seddon, A. (1990) The identification of a second cell cycle control on the HO promoter in yeast: cell cycle regulation of *SW15* nuclear entry. *Cell* 62: 631–647.

Queralt, E., Lehane, C., Novak, B. and Uhlmann, F. (2006) Downregulation of PP2A(Cdc55) phosphatase by separase initiates mitotic exit in budding yeast. *Cell* 125: 719–732.

Reinke, A., Chen, J. C, Aronova, S. and Powers, T. (2006) Caffeine targets TOR complex I and provides evidence for a regulatory link between the FRB and kinase domains of Tor1p. *J. Biol. Chem.* 281: 31616–31626.

Romá-Mateo, C., Ríos, P., Tabernero, L., Attwood, T. K. and Pulido, R. (2007) A novel phosphatase family, structurally related to dual-specificity phosphatases, that displays unique amino acid sequence and substrate specificity. *J. Mol. Biol.* 374: 899–909.

Romá-Mateo, C., Sacristán-Reviriego, A., Beresford, N. J., Caparrós-Martín, J. A., Culiáñez-Macià, F. A., Martín, H., Molina, M., Tabernero, L. and Pulido, R. (2011) Phylogenetic and genetic linkage between novel atypical dual-specificity phosphatases from non-metazoan organisms. *Mol. Genet. Genomics* 285: 341–354.

Ronne, H., Carlberg, M., Hu, G. Z. and Nehlin, J. O. (1991) Protein phosphatase 2A in *Saccharomyces cerevisiae*: effects on cell growth and bud morphogenesis. *Mol. Cell. Biol.* 11: 4876–4884.

Sakumoto, N. Mukai, Y., Uchida, K., Kouchi, T., Kuwajima, J., Nakagawa, Y., Sugioka, S., Yamamoto, E., Furuyama, T., Mizubuchi, H., Ohsugi, N., Sakuno, T., Kikuchi, K., Matsuoka, I., Ogawa, N., Kaneko, Y., and Harashima, S. (1999) A series of protein phosphatase gene disruptants in *Saccharomyces cerevisiae*. *Yeast* 15: 1669–1679.

Sakumoto, N., Matsuoka, I., Mukai, Y., Ogawa, N., Kaneko, Y. and Harashima, S. (2002) A series of double disruptants for protein phosphatase genes in *Saccharomyces cerevisiae* and their phenotypic analysis. *Yeast* 19: 587–599.

Sambrook, E.F. and Fritsch, T. M. (1989) Molecular cloning : a laboratory manual *2nd ed. Cold Spring Harb. New York.*

Schweighofer, A., Hirt, H. and Meskiene, I. (2004) Plant PP2C phosphatases: emerging functions in stress signaling. *Trends Plant Sci*. 9: 236–243.

Selby, C. P. and Sancar, A. (1990) Molecular mechanisms of DNA repair inhibition by caffeine. *Proc. Natl. Acad. Sci.* 87: 3522–3525.

Sharmin, D., Sasano, Y., Sugiyama, M. and Harashima, S. (2014) Effects of deletion of different PP2C protein phosphatase genes on stress responses in *Saccharomyces cerevisiae*. *Yeast* 31: 393–409.

Sherman, F. (2002) Getting started with yeast. *Methods Enzymol.* 350: 3–41.

Shi, Y. (2009) Serine/threonine phosphatases: mechanism through structure. *Cell* 139: 468–484.

Shu, Y., Yang, H., Hallberg, E. and Hallberg, R. (1997) Molecular genetic analysis of Rts1p, a B' regulatory subunit of *Saccharomyces cerevisiae* protein phosphatase 2A. *Mol. Cell. Biol.* 17: 3242–3253.

Sikorski, R. S. and Hieter, P. (1989) A System of Shuttle Vectors and Yeast Host Strains Designed for Efficient Manipulation of DNA in *Saccharomyces cerevisiae*. *Genetics* 122: 19–27.

Sneddon, A. A., Cohen, P. T. and Stark, M. J. (1990) *Saccharomyces cerevisiae* protein phosphatase 2A performs an essential cellular function and is encoded by two genes. *EMBO J.* 9: 4339–4346.

Spellman, P. T., Sherlock, G., Zhang, M. Q., Iyer, V. R., Anders, K., Eisen, M. B., Brown, P. O., Botstein, D. and Futcher, B. (1998) Comprehensive Identification of Cell Cycle-regulated Genes of the Yeast *Saccharomyces cerevisiae* by Microarray Hybridization. *Mol. Biol. Cell* 9: 3273–3297.

Sugiyama, M., Ikushima, S., Nakazawa, T., Kaneko, Y. and Harashima, S. (2005) PCR-mediated repeated chromosome splitting in *Saccharomyces cerevisiae*. *Biotechniques* 38: 909–914.

Sutton, A., Immanuel, D. and Arndt, K. T. (1991) The *SIT4* protein phosphatase functions in late G1 for progression into S phase. *Mol. Cell. Biol.* 11: 2133–2148.

Tate, J. J. and Cooper, T. G. (2007) Stress-responsive Gln3 localization in *Saccharomyces cerevisiae* is separable from and can overwhelm nitrogen source regulation. *J. Biol. Chem.* 282: 18467–18480.

Tate, J. J., Feller, A., Dubois, E. and Cooper, T. G. (2006) *Saccharomyces cerevisiae* Sit4 phosphatase is active irrespective of the nitrogen source provided, and Gln3

phosphorylation levels become nitrogen source-responsive in a sit4-deleted strain. *J. Biol. Chem.* 281: 37980–37992.

Tate, J. J., Georis, I., Feller, A., Dubois, E. and Cooper, T. G. (2009) Rapamycin-induced Gln3 dephosphorylation is insufficient for nuclear localization: Sit4 and PP2A phosphatases are regulated and function differently. *J. Biol. Chem.* 284: 2522–2534.

Uhrig, R. G., Labandera, A. M. and Moorhead, G. B. (2013) Arabidopsis PPP family of serine/threonine protein phosphatases: many targets but few engines. *Trends Plant Sci.* 18: 505–513.

Unnikrishnan, I., Miller, S., Meinke, M. and LaPorte, D. C. (2003) Multiple positive and negative elements involved in the regulation of expression of *GSY1* in *Saccharomyces cerevisiae*. *J. Biol. Chem.* 278: 26450–26457.

Venter, J. C. Adams, M. D., Myers, E. W., Li, P. W., Mural, R. J., Sutton, G. G., Smith, H. O., Yandell, M., Evans, C. A. Holt, R. A. et al. (2001) The sequence of the human genome. *Science* 291: 1304–1351.

Wang, H., Wang, X. and Jiang, Y. (2003) Interaction with Tap42 is required for the essential function of Sit4 and type 2A phosphatases. *Mol. Biol. Cell* 14: 4342–4351.

Wang, Y. and Burke, D. J. (1997) Cdc55p, the B-type regulatory subunit of protein phosphatase 2A, has multiple functions in mitosis and is required for the

kinetochore/spindle checkpoint in Saccharomyces cerevisiae. *Mol. Cell. Biol.* 17: 620–626.

Wanke, V., Cameroni, E., Uotila, A., Piccolis, M., Urban, J., Loewith, R. and De Virgilio, C. (2008) Caffeine extends yeast lifespan by targeting TORC1. *Mol. Microbiol.* 69: 277–285.

Watanabe, D., Wu, H., Noguchi, C., Zhou, Y., Akao, T. and Shimoi, H (2011) Enhancement of the initial rate of ehanol fermentation due to dysfunction of yeast stress reponse components Msn2p and/or Msn4. *Appl. Environ. Microbiol*. 77: 934-941.

Whitmarsh, A. J. and Davis, R. J. (2000) Regulation of transcription factor function by phosphorylation. *Cell. Mol. Life Sci.* 57: 1172–1183.

Yan, G., Shen, X. and Jiang, Y. (2006) Rapamycin activates Tap42-associated phosphatases by abrogating their association with Tor complex 1. *EMBO J.* 25: 3546–3555.

Zolnierowicz, S. and Bollen, M. (2000) Protein phosphorylation and protein phosphatases. *EMBO J.* 19: 483–488.

Van Zyl, W., Huang, W., Sneddon, A. A., Stark, M., Camier, S., Werner, M., Marck, C., Sentenac, A. and Broach, J. R. (1992) Inactivation of the protein phosphatase 2A regulatory subunit A results in morphological and transcriptional defects in *Saccharomyces cerevisiae*. *Mol. Cell. Biol.* 12: 4946–4959.

List of publications

Publications related in this thesis

1. **Numamoto, M., Sasano, Y., Hirasaki , M., Sasano, Y., Sugiyama, M., Maekawa, H., and Harashima, S.:** The protein phosphatase Siw14 controls caffeine-induced nuclear localization and phosphorylation of Gln3 via the type 2A protein phosphatases Pph21 and Pph22 in *Saccharomyces cerevisiae*, *J. Biochem.*, 157, 53-64 (2015).

2. **Numamoto, M., Tagami, S., Ueda, Y., Imabeppu, Y., Sasano, Y., Sugiyama, M., Maekawa, H., and Harashima, S.:** Nuclear localization domains of GATA activator Gln3 are required for transcription of target genes through dephosphorylation in *Saccharomyces cerevisiae*, *J. Biosci. Bioeng.*, doi:10.1016/j.jbiosc.2014.12.017 (available online 29 January 2015).

Other publications

1. **Hirasaki, M., Nakamura, F., Yamagishi, K., Numamoto, M., Shimada, Y., Uehashi, K., Muta, S., Y., Sugiyama, M., Kaneko, Y., Kuhara, S., and Harashima, S.:** Deciphering cellular functions of protein phosphatases by comparison of gene profiles in *Saccharomyces cerevisiae*, *J. Biosci. Bioeng.*, 109, 433-441 (2010).

2. **Hirasaki, M., Horiguchi, M., Numamoto, M., Y., Sugiyama, M., Kaneko, Y. and Harashima, S.:** *Saccharomyces cerevisiae* protein phosphatase Ppz1 and protein kinases Sat4 and Hal5 are involved in the control of subcellular localization of Gln3 by regulating its phosphorylation state, *J. Biosci. Bioeng.*, 111, 249-254 (2011).

Acknowledgements

I would like to express my deepest and sincere gratitude to Professor Satoshi Harashima for his kindness in giving me the great opportunity to study the yeast genetics and molecular biology in his laboratory, and for worthy guidance throughout this study. I would like to thank Assistant Professor Yu Sasano and Associate Professor Minetaka Sugiyama for their helpful comments and supporting during this study. I also express my sincere thanks to Professor Yoshinobu Kaneko and Assistant Professor Hiromi Maekawa (Yeast Genetic Resources Laboratory, Osaka university), for their fruitful discussion. I also thank Assistant Professor Masataka Hirasaki (Division of developmental biology, Saitama Medical University), for his support during the conduct of this study. My appreciation is also expressed to Shigenori Kanaya and Takuya Nihira for their valuable comments and suggestions.

My gratitude is also extended to all Harashima lab members. Special thanks are given to Mr. Shota Tagami, Mr. Yusuke Ueda and Mr. Yusuke Imabbepu for construction of multiple plasmids and analysis of the intracellular localization of Gln3. I owe my thanks to my parents, husband, and children for their encouragement, understanding, and support.